Geomorphology 232 (2015) 164–181

Contents lists available at ScienceDirect

Geomorphology

journal homepage: www.elsevier.com/locate/geomorph

Neotectonic reactivation of the western section of the Malargüe fold and thrust belt (Tromen volcanic plateau, Southern Central Andes)

Lucía Sagripanti [a,*], Emilio A. Rojas Vera [a], Guido M. Gianni [a], Andrés Folguera [a], Jonathan E. Harvey [b], Marcelo Farías [c], Victor A. Ramos [a]

[a] Laboratorio de Tectónica Andina, Instituto de Estudios Andinos "Don Pablo Groeber" (IDEAN), Universidad de Buenos Aires — CONICET, Argentina
[b] Earth Science Department of the University of Santa Barbara — California (UCSB), United States
[c] Departamento de Geología, FCFM, Universidad de Chile, Santiago,Chile

ARTICLE INFO

Article history:
Received 16 October 2013
Received in revised form 1 December 2014
Accepted 4 December 2014
Available online 18 December 2014

Keywords:
Neotectonics
Fluvial pattern
Southern Central Andes geomorphology
Retroarc volcanism
Magnetotellurics
Asthenospheric anomaly

ABSTRACT

This study examines the neotectonic deformation and development of the Tromen massif, a Quaternary retroarc volcanic field located in the western section of the Malargüe fold and thrust belt in the Southern Central Andes. The linkages between neotectonic deformation in the intra-arc zone and the recent retroarc structures of the Tromen volcanic plateau are not clearly understood. These retroarc deformations affect the mid-section of the fold and thrust belt, leaving to the east a 200 km-wide deformed zone that can be considered inactive over the last 12–10 Ma. This out-of-sequence deformation west of the orogenic front area has not been previously addressed in detail. In this study, exhaustive mapping is used to describe and discriminate structures with a neotectonic component from those fossilized by Pleistocene strata. Two balanced cross-sections are constructed showing the distribution of the youngest deformations and their relation to pre-Miocene structures. An important means for evaluating this is the morphometric and morphological analyses that allowed identification of perturbations in the fluvial network associated with active structures. In a broader perspective, neotectonic activity in the fold and thrust belt is discussed and inferred to be caused by local mechanical weakening of the retroarc zone, due to injection of asthenospheric material evidenced by magnetotelluric surveys. Thus, deformation imposed by the oblique convergence between South American and Nazca plates, while to the south being limited to the Liquiñe-Ofqui fault system that runs through the arc zone, in the retroarc area is located at the site of magmatic emplacement, presumably in association with a thermally weakened-upper crust. This control exemplifies the relationship that exists between surficial processes, magmatic emplacement and upper asthenospheric dynamics in the Southern Central Andes.

1. Introduction

The Southern Central Andes are the result of the steady displacement of South America since 100 Ma, when it started a westward drift after its separation to the rest of Gondwana (Oncken et al., 2003; Kay et al., 2006; Charrier et al., 2007; Somoza and Zaffarana, 2008; DeCelles et al., 2009; Somoza and Ghidella, 2012). However, morphological variations along strike, potentially associated with variable tectonic settings and a shortening gradient, are still extensively discussed (Kley et al., 1999; Ramos et al., 2004; Ramos, 2010). Even though most of the eastern Andean foothills record contractional deformation, as indicated by geological, seismological and geodetic evidence (Kendrick et al., 1999; Brooks et al., 2003; Costa et al., 2006; Guzmán et al., 2007; Farías et al., 2010), some segments have accommodated limited amounts of extension recently and during previous stages of Andean development (Jordan et al., 2001; Pananont et al., 2004; Folguera et al., 2006; Charrier et al., 2007; Lagabrielle et al., 2007; Rojas Vera et al., 2014).

This study is focused in the Andean retroarc zone at 36–37°S, as part of the Southern Volcanic Zone (Jordan et al., 1983; Ramos and Aleman, 2000). This sector, located to the west of the orogenic front area, has been the locus of extensive debate about its present mechanisms of deformation (Galland et al., 2007; Folguera et al., 2008; Messager et al., 2010). South of 38°S, the intra-arc zone is characterized by a neotectonic system known as the Liquiñe Ofqui fault system (LOFS) (Fig. 1) that runs through the present volcanic arc (López-Escobar et al., 1995; Lavenu and Cembrano, 1999; Cembrano et al., 2002). The LOFS is considered one of the longest active, dextral strike-slip fault systems in a subduction zone, and has been developed since the late Miocene in relation to the oblique convergence between the Nazca and South American plates (Fig. 1) (Quezada and Bataille, 2008; Cembrano and Lara, 2009).

* Corresponding author.
E-mail address: lusagripanti@gmail.com (L. Sagripanti).

http://dx.doi.org/10.1016/j.geomorph.2014.12.022
0169-555X/

Its right-lateral kinematics are revealed by focal mechanisms, kinematic analyses and limited morphotectonic indicators (Lavenu and Cembrano, 1999; Quezada and Bataille, 2008). A series of NNE lineaments, faults and ductile-shear zones, define two major NNE-trending segments joined by a series of *en-echelon* faults at a right step (Lavenu and Cembrano, 1999). This fault system projects locally into the eastern slope of the Southern Central Andes, crossing the axial mountain sector north of 38°S and continuing in the western retroarc area as the Antiñir-Copahue fault system (ACFS) for more than 200 km next to the drainage divide area at the latitudes of the study area (Radic et al., 2002; Folguera et al., 2004; Melnick et al., 2006) (Figs. 1, 2).

The Antiñir-Copahue fault system (ACFS; Figs. 1, 2) deforms Miocene to Quaternary rocks in a narrow belt parallel to the drainage divide area, accommodating right-lateral displacements and contraction (Folguera et al., 2004, 2006). Even though less than 6 ka-old mass wasting deposits, late Pleistocene fluvio-glacial terraces and soil horizons are deformed through this system, the main deformational stage is ascribed to the 1.7–1.4 Ma interval (Folguera et al., 2004, 2006; Folguera and Ramos, 2009; Hermanns et al., 2011; Penna et al., 2011). Contrastingly, to the east, the Malargüe and Agrio fold and thrust belts had mostly been considered fossilized in the last ~12–10 Ma in terms of contractional deformation (Fig. 2). These deformational belts had a period of construction that started in the Late Cretaceous–Eocene, with a reactivation in late Miocene times, evidenced by synorogenic deposits, cross-cutting relationships and limited amounts of fission track data (Ramos, 1998; Zamora Valcarce et al., 2006, 2009; Rojas Vera et al., 2014).

This work analyzes a neotectonic system located in the western slope of the Tromen volcanic plateau that runs through the retroarc zone affecting the western Malargüe fold and thrust belt (Fig. 1, 2), initially distinguished by Galland et al. (2007) as a Quaternary compressional system.

Through detailed mapping, we reconstruct the deformational history of this area and relate young deformation to the reactivation of previous contractional structures of the Malargüe fold and thrust belt. Two structural cross-sections show the exact distribution of the Cretaceous to Miocene contractional structures and their local neotectonic reactivation. Perturbations to the fluvial network produced by these neotectonic reactivations in the retroarc zone were analyzed through morphometric and morphological analysis.

Finally, retroarc neotectonic deformation is discussed in a more regional context, with respect to its location within the fold and thrust belt and potential lithospheric and sublithospheric controls.

2. Tectonic framework

The retroarc zone north of 38°S is characterized by the extensive development of intra-plate series of the Payenia volcanic plateau (Fig. 2) (Jordan et al., 1983; Kay et al., 2006; Llambías et al., 2010; Ramos and Folguera, 2011; Kay et al., 2013; Søager et al., 2013). Recent 3D inversion of magnetotelluric (MT) array data finds that this backarc volcanism is closely associated with the impact of a mantle plume beneath the South American lithosphere (Burd et al., 2008, 2014) (Fig. 2).

The Tromen volcanic plateau constitutes the westernmost part of this magmatic province, partly superimposed on the Malargüe fold and thrust belt compressional structures (Fig. 2) (Zollner and Amos, 1973; Holmberg, 1975). There are two conductive anomalies described by Burd et al. (2014): an eastern one (see Fig. 2), called the DEEP (DEep Eastern Plume) in this study because it has a source area below 300 km although it appears to rise locally above 30 km (see Fig. 2); and a second one, further west, called the SWAP (Shallow Western Asthenospheric Plume). The last has chimneys rising directly beneath the western Tromen volcanic plateau and near Payun Matru. The DEEP and the SWAP are not currently connected, although Burd et al. (2014) suggest that during Miocene shallow subduction the SWAP and the DEEP were a unique plume. Subsequently, as the slab steepened at the beginning of the Pliocene, the shallow mantle flowed westward into the area formerly occupied by the Nazca slab and the SWAP was dragged from the original plume.

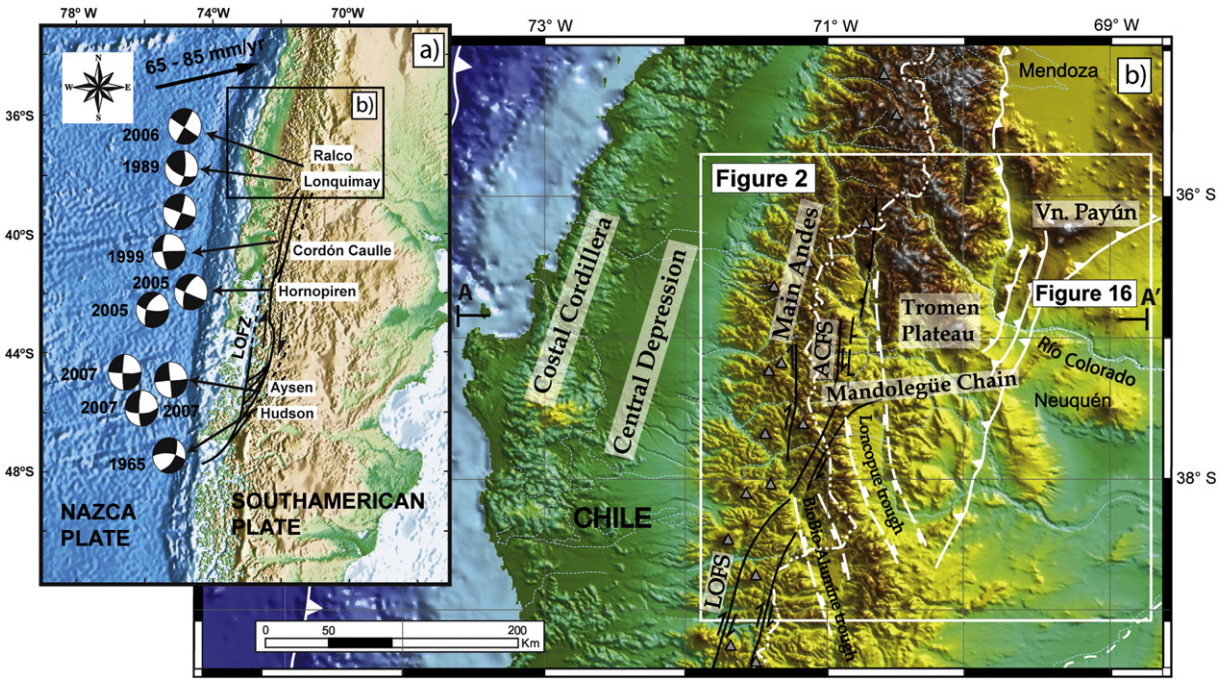

Fig. 1. a) Southern Central and Patagonian Andes and distribution of neotectonic deformation (indicated with black lines) concentrated in the Liquiñe Ofqui fault system (LOFS), running through the arc front. Note that crustal seismicity implies a dextral strike-slip kinematics (Quezada and Bataille, 2008; Cembrano and Lara, 2009). b) Main morphostructural units in the study area in the southernmost Southern Central Andes. Note that the LOFS crosses the drainage divide area affecting the eastern Main Andes at the Antiñir-Copahue fault system (ACFS) (Folguera et al., 2004; Rojas Vera et al., 2008, 2014). The Tromen volcanic plateau is located to the east of the ACFS.

The Tromen volcanic plateau had its major period of activity between Pleistocene and Holocene (Fig. 3) (Zollner and Amos, 1973; Holmberg, 1975; Llambías et al., 1982), although there are some historical eruptions reported in 1752 and 1822 (Havestadt, 1752; Siebert et al., 2011). It is associated with rhyolitic domes and lava and pyroclastic flows with ages ranging from 2.3 to 0.8 Ma, plus mafic to mesosilicic lava flows and dyke complexes with ages ranging from 1.9 to 0.04 Ma (Fig. 3a). Geochemical data have shown that most of the sequence forming the Tromen volcanic section comes from typical within-plate melts, with no connection to the subducted oceanic slab, and that only the basal products around 4 Ma would have had an arc affinity (Kay, 2002; Kay et al., 2006; Galland et al., 2007). The entire volcanic section of the volcanic plateau lies unconformably upon the deformed Mesozoic and Paleocene to Miocene successions (Zollner and Amos, 1973; Kozlowski et al., 1996; Zapata et al., 1999).

The Malargüe fold and thrust belt has been formed by the inversion of Late Triassic–Early Jurassic depocenters of the Neuquén Basin (Kozlowski et al., 1993; Vergani et al., 1995). A dominant thick-skinned style of deformation is locally associated with thin-skinned deformational sectors, represented by complex structures detached in marine sediments of the Auquilco and Vaca Muerta Formations (Middle to Late Jurassic–Early Cretaceous), and evaporitic deposits of the Huitrín Formation (Early Cretaceous) (Zamora Valcarce et al., 2006; Rojas Vera et al., 2014). In particular, the Tromen volcanic plateau is partly superimposed on a basement contractional structure that exhumes

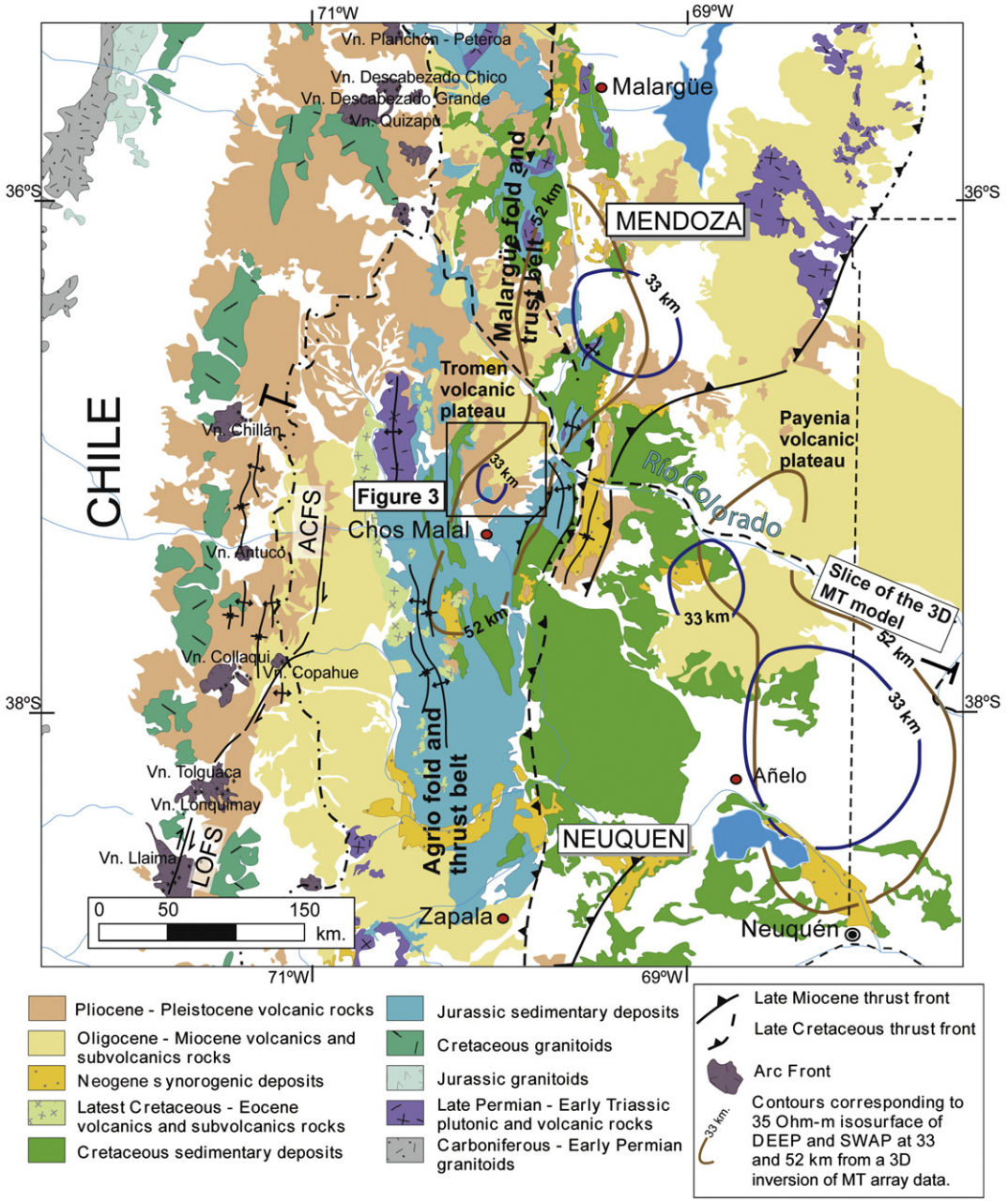

Fig. 2. Geology of the southernmost Southern Central Andes and indication of the study area in the Tromen volcanic plateau. The Main Andes exposes late Oligocene to early Miocene volcanic rocks and sedimentary successions unconformably overlain by Pliocene to Quaternary arc-derived rocks. To the east, the Malargüe and Agrio fold and thrust belts deform Early Triassic to Late Cretaceous sedimentary deposits of the Neuquén Basin. North of 38°S, the retroarc zone is characterized by profuse Quaternary eruptions forming the Payenia volcanic plateau in which the Tromen volcanic plateau is located. Crustal and upper-mantle contours of resistivity derived from 3D inversion of MT array data, are interpreted as a mantle plume impacting the lower crust coincident with these retroarc eruptions at the surface (see text for further details) (Burd et al., 2014).

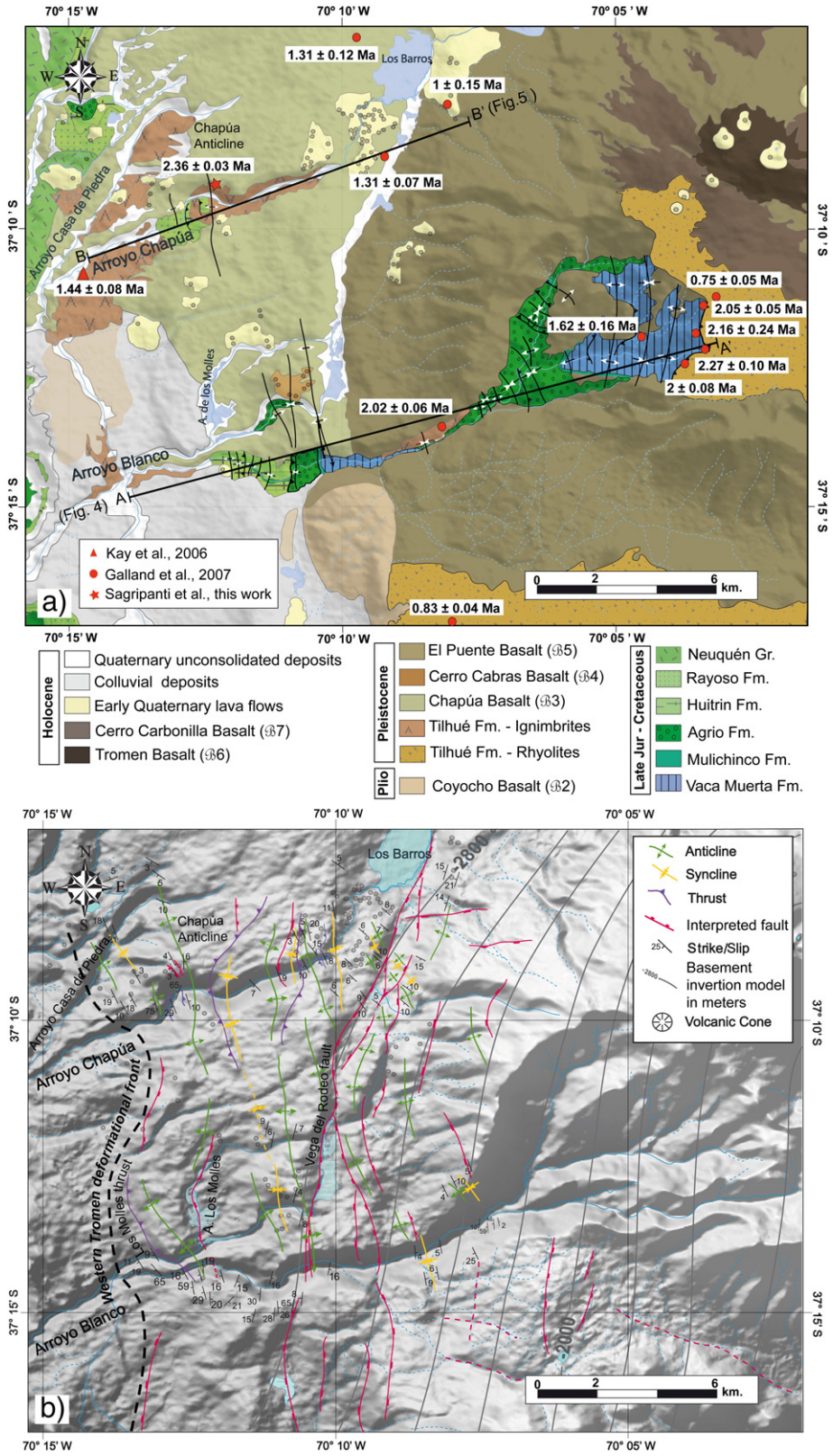

Fig. 3. a) Geology of the western Tromen volcanic plateau. Mesozoic deposits of the Neuquén basin are exposed at the Arroyo Blanco and Arroyo Chapúa. Deformed Mesozoic strata are covered unconformably by late Pliocene to Pleistocene volcanic rocks. Available Ar–Ar ages from Kay et al. (2006), Galland et al. (2007) and this work are shown that constrain these rocks to the 2.3–0.75 Ma interval. b) Identified neotectonic structures, structural data and computed depth of the pre-Mesozoic basement, derived from an inversion of gravity data, are shown (after Sagripanti et al., 2012b). The gravity data show the uplift of a basement block in the east at depth (see text for further details).

Mesozoic sedimentary sequences. This structure is partially and unconformably buried by early Miocene volcanic sections that indicate a pre-Miocene age of exhumation (Spagnuolo et al., 2012). However, this plateau is the locus of Quaternary deformation and constitutes the easternmost structures in which deformation is concentrated (Fig. 2) (Galland et al., 2007; Messager et al., 2010). The deformation

described on the western flank of this volcanic complex has been the subject of recent debate. On one hand, it was interpreted as an extensional setting for the basal Tromen plateau lavas based on field and seismic evidence limited to the southern part of the plateau (Folguera et al., 2008). This hypothesis finds a rather coherent justification linked to the proposed steepening of the Nazca plate in the last 5 My, and consequent back-arc extension (Ramos and Folguera, 2005; Ramos and Kay, 2006; Kay et al., 2006; Ramos et al., 2014). On the other hand, it was proposed from field data that certain structures are associated with Quaternary contractional deformation (Marques and Cobbold, 2002; Galland et al., 2007). More recently, Messager et al. (2010) described compressional and subordinate extensional structures that coexisted southwest of the Tromen volcanic plateau. Similarly, trying to resolve these contrasting data, Backé et al. (2006) had proposed that both mechanisms coexisted, generated by strike-slip displacements affecting the western slope of the Tomen volcanic plateau.

3. Methods

Structural field observations were used to define fault geometries at the surface and their temporal development in the area, through the recognition of two general stages of deformation: one pre-dating the Miocene and the other falling within the last ~2 Ma. Shortening extents were calculated to quantify deformation through both stages, using the *Midland Valley software (2D Move)* that allowed restoration to the undeformed stage. Basement and simple detachment structures were modeled and restored using the flexural slip algorithm. In other cases, some localized sectors with more complex deformation were restored using the fault parallel flow (Egan et al., 1997; Kane et al., 1997).

Field observations focused on the Arroyo Chapúa and Arroyo Blanco were complemented with the analysis of ASTER and LANDSAT satellite images in the western slope of the Tromen volcanic plateau (Fig. 3). Additionally, we studied the tectonic geomorphology of the Tromen volcanic plateau using field observations and analysis of digital topography (SRTM — 30 m digital elevation data), focusing on the drainage pattern and stream profiles. A series of NE-orientated, — 10 km long swath profiles were made at regular intervals, showing maximum, mean and minimum topographic values through the western slope of the Tromen volcanic plateau, including the entire zone where most of the neotectonic structures were recognized.

In particular, the drainage network, flow accumulation and flow direction of the drainage were computed with *ArcGIS* software. In order to calculate the longitudinal river profiles, profile concavity, as

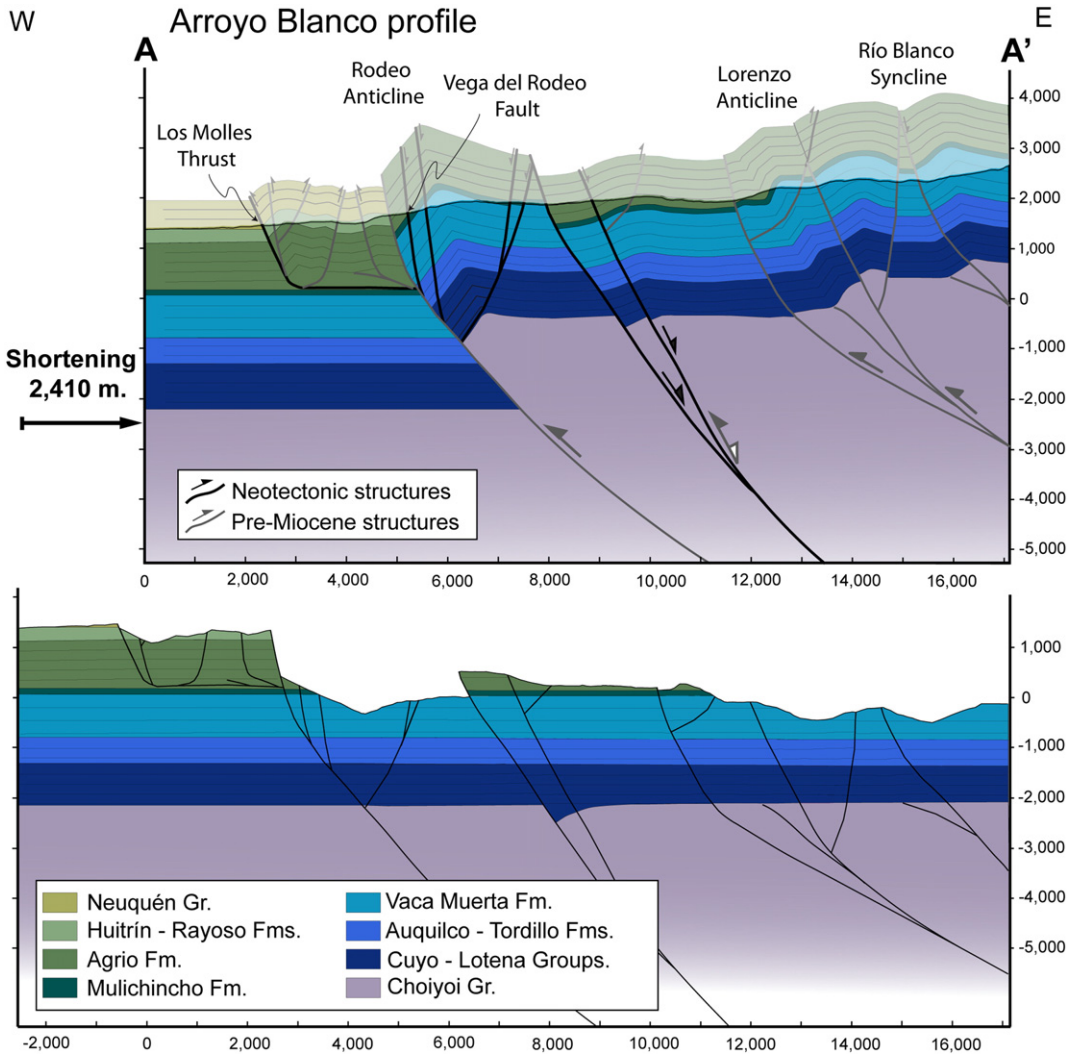

Fig. 4. Structural cross- section and palinspastic restoration along the Arroyo Blanco draining the western slope of the Tromen volcanic plateau (see Fig. 3 for location). A narrow-frontal thin-skinned domain is formed in the west, whose shortening is transferred from a series of basement structures to the east. Note neotectonic reactivations focused in the western deformational front as well as in certain basement structures in the east.

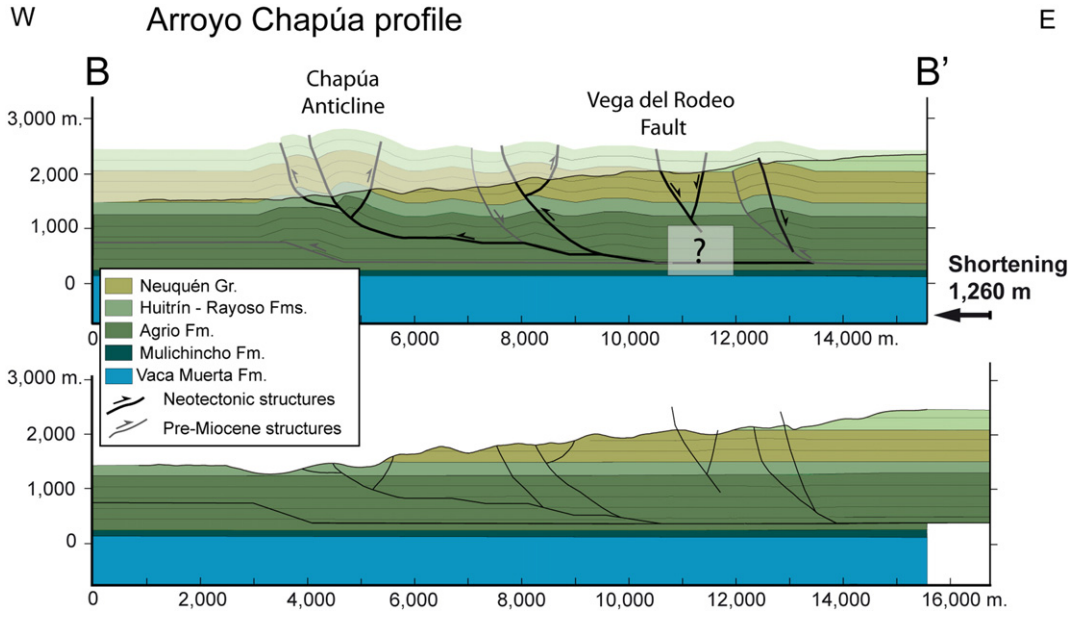

Fig. 5. Structural cross-section and palinspastic restoration along the Arroyo Chapúa that drains the western slope of the Tromen volcanic plateau in the northern study area (see Fig. 3 for location). Note a wider development of the thin-skinned belt in comparison with the Arroyo Blanco profile (see Fig. 4). Note also neotectonic reactivations widely distributed through different structures of this sector.

well as channel normalized steepness indexes (k_{sn}), we used the *Stream Profiler* (available at http://geomorphtools.gor) that operates using *ArcGIS* and *MATLAB*. Transitions in channel slope and knickpoints were marked along the profiles in order to identify possible topographic anomalies that could correlate with regions of potential ongoing rock uplift, following other studies that relate the sensitivity of fluvial networks to active tectonic processes at local and regional scales (Pazzaglia et al., 1998; Keller et al., 1999; Wobus et al., 2006). In this analysis, we assume steady-state river incision into bedrock, and a power-law relation between channel slope (S) and drainage area (A), where k_s and θ are the steepness and concavity indices, respectively (Hack, 1973; Howard and Kerby, 1983; Whipple and Tucker, 1999; Whipple et al., 2000; Wobus et al., 2006).

$$S = k_s A^{-\theta} \quad (1)$$

The concavity index (θ) is relatively insensitive to differences in rock uplift rate, climate and substrate lithology at steady state, although the steepness index (k_s) varies with them (Kirby and Whipple, 2001; Wobus et al., 2006; Kirby and Whipple, 2012), constituting a useful metric for tectonic geomorphic studies. By fitting linear regressions to log-slope and log-area data evaluating slope-area regression, using a reference concavity index (θ_{ref}), one can determine an along-stream normalized steepness index (k_{sn}) that allows effective comparison of the profiles of the different streams with greatly varying drainage area (Kirby and Whipple, 2001; Wobus et al., 2006; Kirby and Whipple, 2012). The relationship between k_s and uplift is widely accepted, although as mentioned, it is strongly influenced by geologic setting and climate (Wobus et al., 2006). Since uplift tends to steepen rivers, the steepness index should vary in response (Snyder et al., 2000). Therefore, Eq. (1) is a useful tool to extract information on regional tectonics and on uplift patterns (Kirby and Whipple, 2001; Wobus et al., 2006).

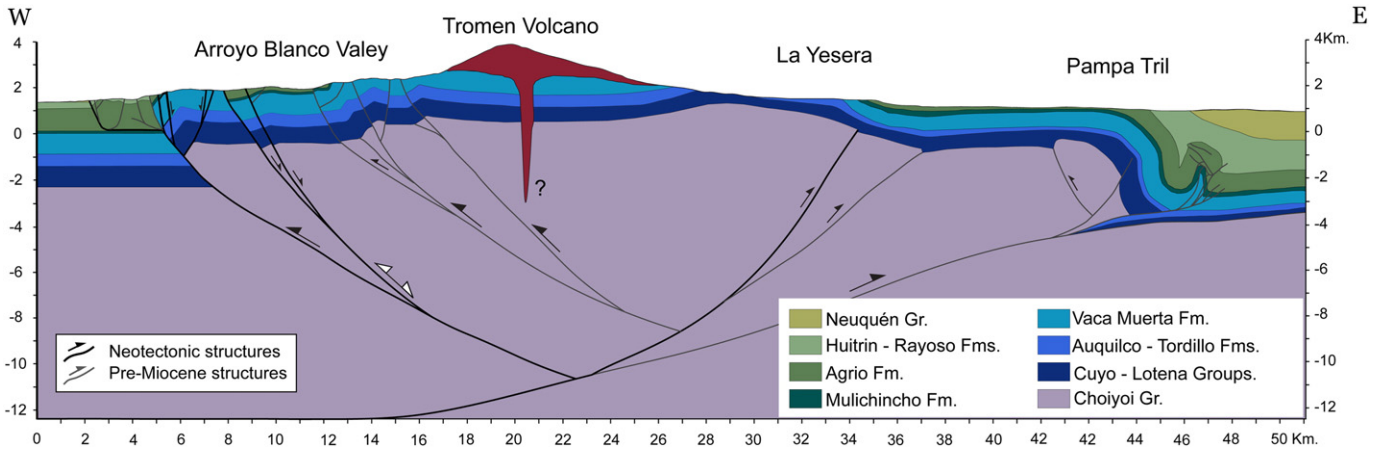

Fig. 6. Regional cross- section across the Tromen volcanic plateau that compiles our data and previous works (La Yesera and Pampa Tril structures at depth are constructed from seismic and field information of Zamora Valcarce and Zapata (2005) and Galland et al. (2007)). The overall structure constitutes a doubly-vergent system associated with an east-vergent wedge at depth, over which a series of backthrusts and the thrust associated with La Yesera anticline (Messager et al., 2010) concentrate neotectonic reactivations.

The concavity index (θ) is the slope of the regression line in LogS-LogA space. The streams that reach an equilibrium state are characterized by a concave-upward shape and consequently will have a positive concavity index, whereas rivers in tectonically active areas may exhibit convex profiles. Even rapidly uplifting rivers should eventually produce a concave profile, the convexity comes where two concave segments meet at a knickpoint or where a single river moves into a zone of rapid rock uplift part-way along its profile (Kirby and Whipple, 2001; Burbank and Anderson, 2012).

4. Results

4.1. Geology and structural data of the western Tromen volcanic plateau

Detailed field work performed on the western slope of the Tromen volcanic plateau reveals multiple deformational stages. Most of the identified contractional structures lie unconformably beneath the Pleistocene volcanic rocks (Fig. 3a). However, part of the contractional structure, is affecting the youngest, ~2–1 Ma sections of the volcanic plateau (Fig. 3b). The combination of these deformational events generated a predominantly west-vergent fan of thrusts and folds with variable amplitude.

The Mesozoic basement of the Tromen volcanic plateau is only exposed through two valleys, the Arroyo Blanco in the south and Arroyo Chapúa in the north, where field work was partly concentrated (Fig. 3a). The Arroyo Blanco drains the entire western slope of the Tromen volcanic plateau, incising up to the Early Cretaceous sections. Downstream, a western Tromen deformational front is recognized, where a NW-trending anticline deforms ~1.4–1.9 Ma volcanic rocks (Fig. 3b) (Galland et al., 2007), emplaced unconformably over late Early Cretaceous sequences that show a greater deformation (Fig. 3a). To the east, a series of short wave-length N- to NNW-trending anticlines and synclines affects Middle to Early Cretaceous sections at a similar exhumation level (Fig. 4). This trend is interrupted by a thrust associated with the long wavelength Rodeo anticline that exhumes Early Cretaceous rocks (Fig. 4). A normal fault cross-cuts the backlimb of this structure, creating a small depocenter filled by Early Quaternary pyroclastic deposits interbedded with fluvial packages. Upstream, in the headwaters of the Arroyo Blanco, N-trending highly asymmetric folds characterized by long wave-lengths (Lorenzo anticline and Arroyo Blanco syncline, among others), expose Late Jurassic to Early Cretaceous successions unconformably beneath andesitic to rhyolitic rocks of the Tilhue Formation (~0.8 to 2.2 Ma) (Galland et al., 2007) (Figs. 3a, 4).

This change from narrow contractional structures in the west to long wave-length structures in the east coincides with a strong gradient in gravity anomalies that implies a shallowing of the basement rocks, as depicted in Fig. 3b (Sagripanti et al., 2012b). This is interpreted as the result of uplift of the Paleozoic basement beneath the Mesozoic sections in the eastern part of the Tromen volcanic plateau.

A structural cross-section through the Arroyo Blanco (Figs. 3a, 4) was constructed in order to describe the shortening and discriminate between pre-Miocene and neotectonic structures. Total shortening is assessed at 2.41 km and can simply be explained by the activity of west-verging basement thrusts and a frontal thin-skinned sector with variable amplitude (Fig. 4). Westernmost basement structures are connected to this thin-skinned frontal sector through its insertion beneath the Early Cretaceous sections (Fig. 3a). To the east, anticlines are controlled by a deeper decollement in the basement. Superimposed extensional deformation also develops east of this point of insertion (Figs. 3, 4).

To the north, along the Arroyo Chapúa, the erosional levels are considerably shallower (Fig. 3a). Most of the structures affect late Early Cretaceous sections and Pliocene to Quaternary pyroclastic and

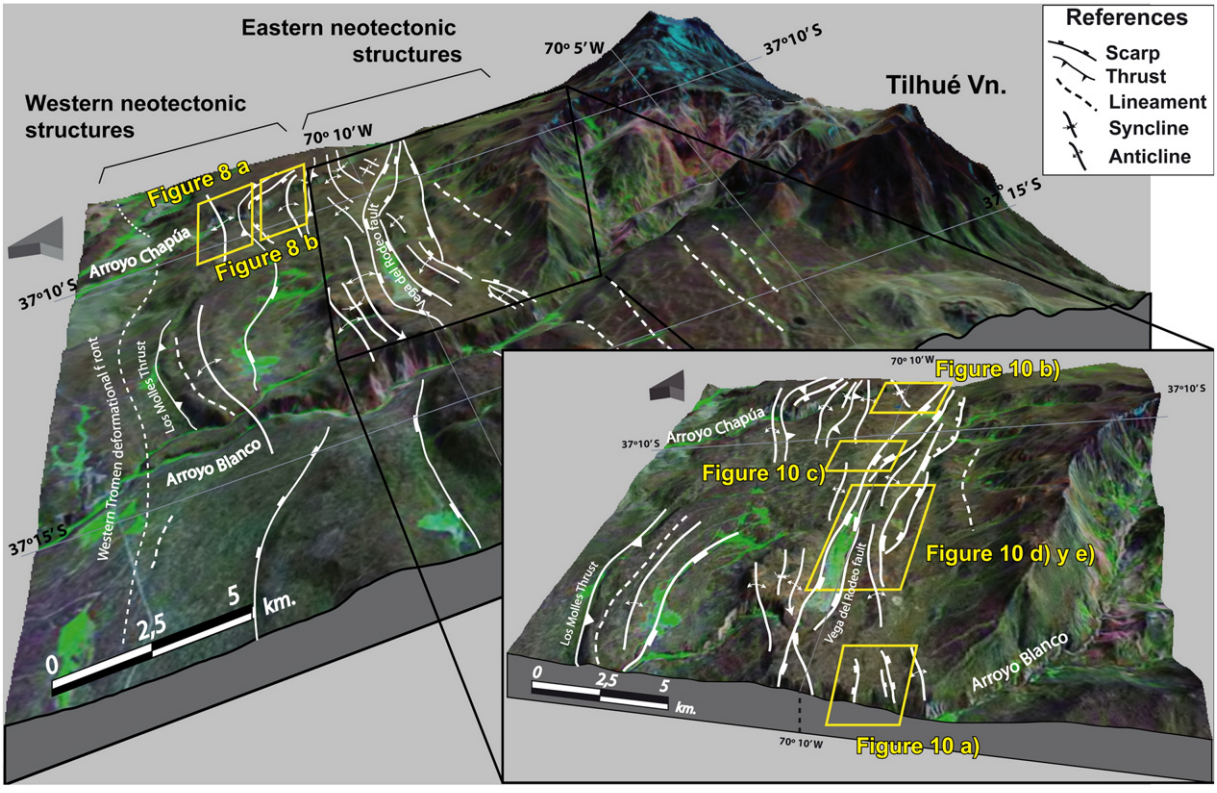

Fig. 7. Block diagram of a TM image draped on top of a DEM, of the western slope of the Tromen volcanic plateau where western and eastern neotectonic structures are shown. In the lower right corner a detail of the eastern neotectonic structures is represented.

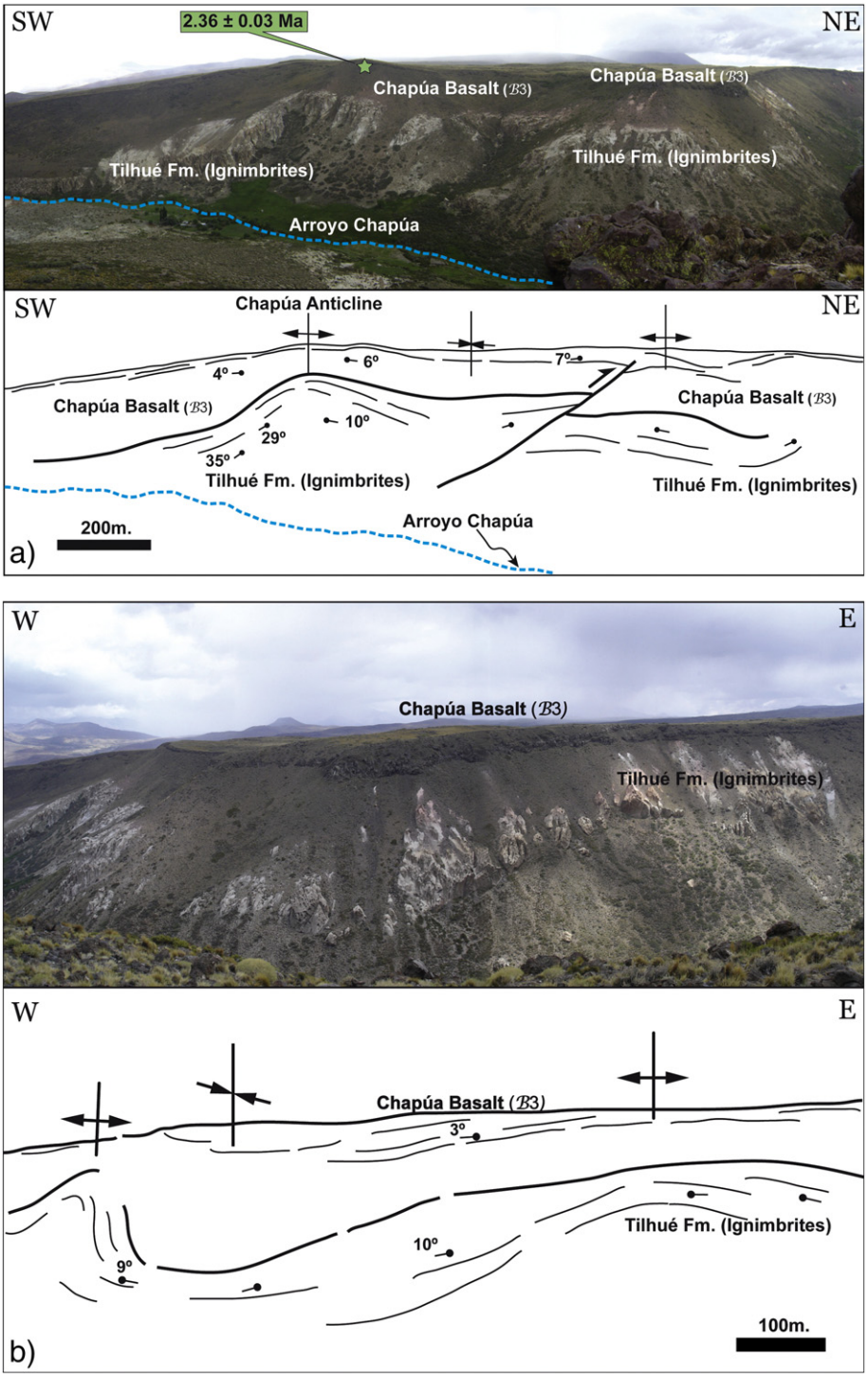

Fig. 8. a) Chapúa Anticline in the western Arroyo Chapúa, affecting the Pleistocene Chapúa Basalt (Ar–Ar 2.36 ± 0.03 Ma; this work) and lower ignimbrites assigned to the earliest Pleistocene Tilhué Formation. b) Other neotectonic structures developed upstream of (a). Note an unconformity between the two Pleistocene volcanic sections, which indicates one long, continuous stage of deformation throughout the Pleistocene that shaped the deformational front (see location in Fig. 7).

lava flows at the surface. A structural cross-section shows a series of short wave-length structures interpreted as part of a thin-skinned deformational belt that accommodates 1.26 km of shortening (Fig. 5). The cross-section shows that this sector would detach in the Early Cretaceous Agrio Formation (Fig. 5).

The Chapúa anticline is the westernmost structure along this trend exposing Mesozoic sections at its core (Galland et al., 2007) (Figs. 3b, 5). This anticline has a west-vergence, with frontal- and back-limbs dipping 35°–29°W and 10°E, respectively, locally interrupted by a reverse fault. To the east, a broad deformational belt that affects Quaternary volcanic rocks, southwest of Los Barros lake, is interrupted by the NE-trending Vega del Rodeo fault (Figs. 3b, 5). This structure branches into a series of minor synthetic traces that define the alternation of topographic lows and highs. Along this area, Pleistocene cover is deformed into a series of *en echelon* anticlines and synclines (Fig. 3b).

From a more regional perspective, the Tromen volcanic plateau is emplaced over the aforementioned array of backthrusts (Fig. 6).

In contrast, the eastern slope of this uplift is marked by the east-verging La Yesera and Pampa Tril basement contractional structures whose last stage of development is inferred to be Late Neogene (Fig. 6) (Zamora Valcarce and Zapata, 2005). Inferred structure at depth suggests a double-vergent basement structure, generated by an east-verging basement wedge (Fig. 6).

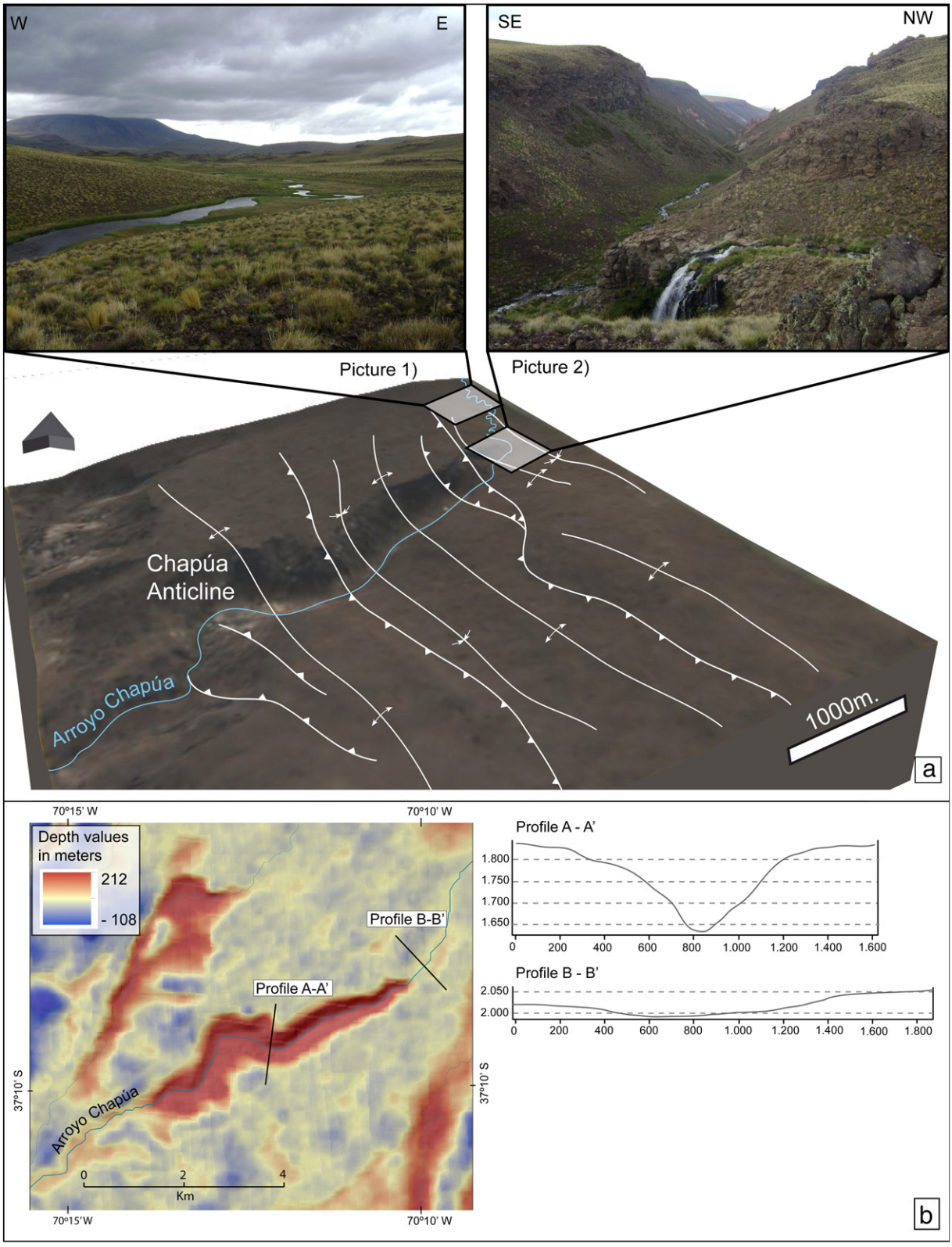

Fig. 9. a) Block diagram showing the relationship between neotectonic structures in the Arroyo Chapúa and changes in the channel morphology. Upstream the Arroyo Chapúa is characterized by a meandering morphology, while downstream, after crossing a neotectonic structure, it becomes incised 200 m in less than 2000 m — acquiring a straighter morphology (transverse profiles A and B show contrasting morphologies of the Arroyo Chapúa downstream and upstream respectively). b) Digital depth model with values highlighting the areas with greater incision.

4.2. Description of the neotectonic structure and fluvial pattern

Neotectonic structures are identified affecting Pleistocene strata in two discrete areas through the western slope of the Tromen volcanic plateau (Fig. 7). The Western neotectonic structures coincide with the Tromen deformational front at the lowest part of the volcanic flank, and are formed by a narrow strip of NNW-trending anticlines, with a west-vergence associated with a frontal thrust.

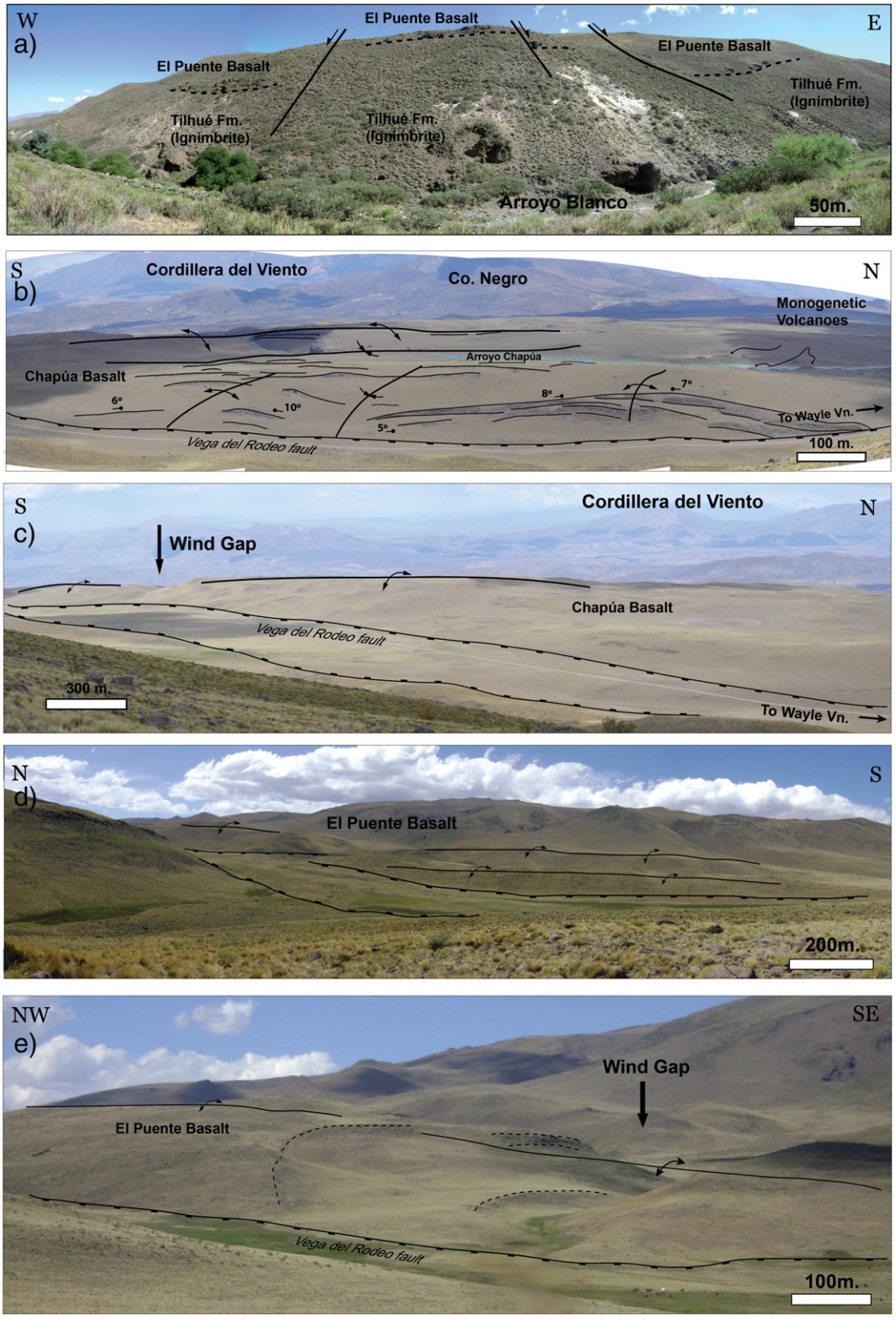

Fig. 10. a) Normal faults affecting Pleistocene basalts and ignimbrites downstream Arroyo Blanco. b) Folding of the Chapúa Basalts at the main topographic break of the western Tromen volcanic plateau. Monogenetic younger volcanism associated with fissures partly fill structural depressions produced during this deformational stage. c) East-facing scarp of the Vega del Rodeo fault associated with an anticline with a wind gap showing a recent uplift. d) Contractional anticlines affecting the Chapúa Basalt alternating with linear scarps outlining axial depressions. e) Wind gap carved in the axial sector of an anticline located between the Arroyo Chapúa and Arroyo Blanco (see location in Fig. 7).

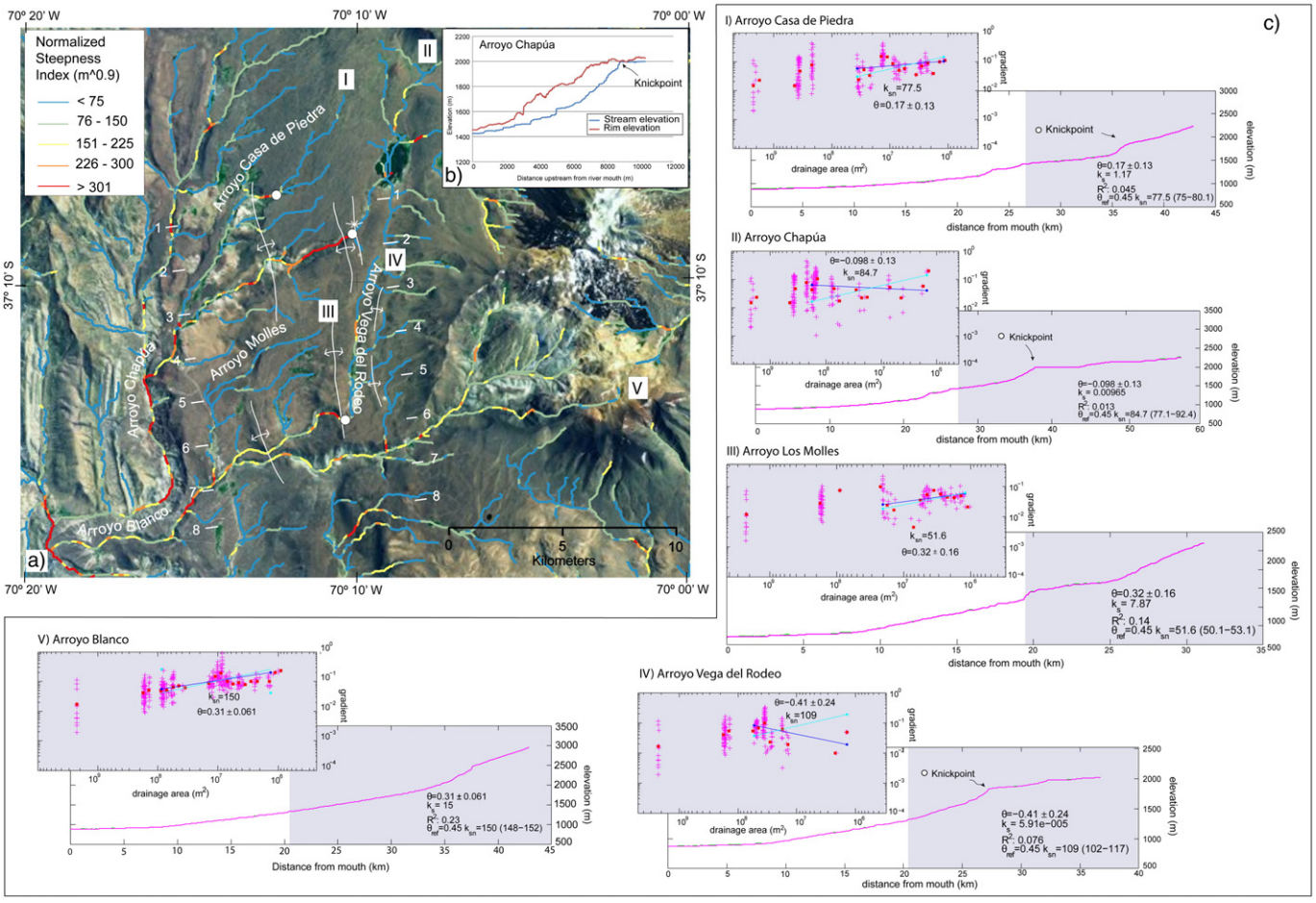

Fig. 11. a) Drainage network at the study area represented by the normalized steepness index (k_{sn}). b) Longitudinal profiles through a rim and the stream of the Arroyo Chapúa, where the rim diverges from the stream profile at a site of recognized neotectonic deformation. c) Longitudinal river profiles of 5 selected streams and tributaries developed over the western slope of the Tromen volcanic plateau. Through each river profile, regression (LogS-LogA) used to calculate concavity is shown independently in the upper left corner (shaded areas on the profiles represent the segments where the regression was made). Note that the profiles I, II, IV show partly convex channels with obvious knickpoints, while profile V is closer to a classic 'graded' profile form (see text for further details).

The western deformational front at the Arroyo Chapúa is defined by two anticlines that deform Pleistocene ignimbritic sheets and unconformable-upper lava flows (Chapúa Basalt) (Fig. 8) (Galland et al., 2007). A new Ar–Ar age obtained in the Chapúa Basalt, near the crest of the Chapúa anticline, has yielded 2.36 ± 0.03 Ma (Fig. 8 and supplementary data). Therefore, based on the aforementioned unconformity, neotectonic shortening could have taken place at least in two stages, starting in the earliest Pleistocene.

The eastern neotectonic structures (Fig. 7) constitute a broader zone of young deformations where N- and NNE-trending normal faults alternate with N- and NNW-trending contractional structures. These structures coincide upstream with an abrupt change in the morphology of the Arroyo Chapúa, from meandering, with a U-shaped valley, to straight downstream with a highly incised V-shaped morphology and a narrow valley (Fig. 9). This change occurs in a step of less than 200 m from the point of intersection of the valley with the easternmost neotectonic structure (Fig. 9). Therefore the valley morphology appears to be sensitive to the described tectonically active area (Figueroa and Knott, 2010).

One of the most important neotectonic structures of this last group in terms of areal development is the Vega del Rodeo fault, which runs through the area of the volcanic plateau interposed between the Arroyo Blanco and the Arroyo Chapúa (Figs. 7, 10). The nature of this fault and other minor associated scarps are revealed where their trace intersects the Arroyo Blanco to the south, where meter-scale displacements in Pleistocene strata are distinguished (Fig. 10a). This fault generates river deflections, wind gaps, small ridges and linear depressions with an *echelon* distribution (Figs. 3, 7, 10b–e). The ridges correspond to neotectonic anticlines slightly limited by scarps (Fig. 10b–e). Sudden terminations of valleys against these scarps and ridges coincide with small endorheic basins associated with springs (Fig. 10e).

Wind gaps and abandoned rivers reflect that the drainage is gradually deflected and defeated by the neotectonic structures of the western slope of the Tromen volcanic plateau. The rivers are forced to change their original course, being in some cases forced to migrate laterally towards the tips of the uplifting areas where they form confluences with transverse rivers (Fig. 10). The diverted drainage system is typically asymmetrical because the defeated rivers are usually diverted towards the nose of the fold, that is, in the direction of fold propagation.

4.3. Morphometric analysis

In this section we analyze the morphology of the area between Arroyo Blanco and Arroyo Chapua and compare it with field observations (Fig. 7), with the aim of recognizing recent deformation and how it affects the fluvial network. As shown in the previous section, the geomorphology of the study area can be divided in two regions with

contrasting topography: A pronounced relief area, where the Tromen volcano is located, and a low-relief area to the west. The drainage pattern reflects these changes: Near the Tromen volcano the drainage predominantly comprises small radial catchments; in the western zone there is a severe reorganization of the drainage network, including wind gaps, dissected rivers, knickpoints and sag ponds. Most of the rivers in this last area are ephemeral channels that only have running water during the rainy seasons (Fig. 11a). Here, a series of alternating ridges and depressions are observed altering the fluvial network. These are produced by Pleistocene deformed volcanic products that determine deflections and wind gaps along the anticline crests.

In order to study potential influences on the fluvial network due to this tectonic activity, we calculated steepness indices and extracted stream profiles of 5 selected channels: tributaries and principal channels (from north to south: I — Arroyo Casa de Piedra, II — Arroyo Chapúa, III — Arroyo Los Molles, IV — Arroyo Vega del Rodeo and V — Arroyo Blanco) (Fig. 11a, c). The longitudinal profiles of these rivers show a general-concave-up shape, although many of them show straight segments and knickpoints (Fig. 11c). Once the knickpoints were identified along the river profiles, the drainage patterns with the corresponding steepness index values are plotted, showing that there exists a strong correlation between the location of the knickpoints and the identified neotectonic structures (Fig. 11a). In particular, along the Arroyo Chapúa, the associated rim profile has a contrasting topography with respect to the stream profile, with a topographic high that is coincident with a knickpoint and laterally related to a young anticline (Fig. 11b).

Concavity values (θ) were calculated along these 5 selected profiles upstream of where these join other major tributaries, regardless of the presence of knickpoints. Negative concavity values indicate a convex profile due to the presence of a large knickpoint along the analyzed segment. Profiles I — Arroyo Casa de Piedra, II — Arroyo Chapúa, and IV — Arroyo Vega del Rodeo present well-developed knickpoints (Fig. 11c). In particular, the I — Arroyo Casa de Piedra shows a dramatic knickzone at around 2000 and 1800 m elevation, with an overall concavity (θ) of 0.17 ± 0.13. Downstream, another convex-upward section and knickpoint are related to the confluence with the Arroyo Chapúa. Likewise, the Arroyo Chapúa to the south has a convex-upward shape, with a concavity (θ) of −0.098, showing a prominent knickpoint at ~2000 m and two other smaller knickpoints downstream at ~1400 and 1200 m elevation. The Arroyo Vega del Rodeo has a marked step around 1900–2000 m, presenting the lowest

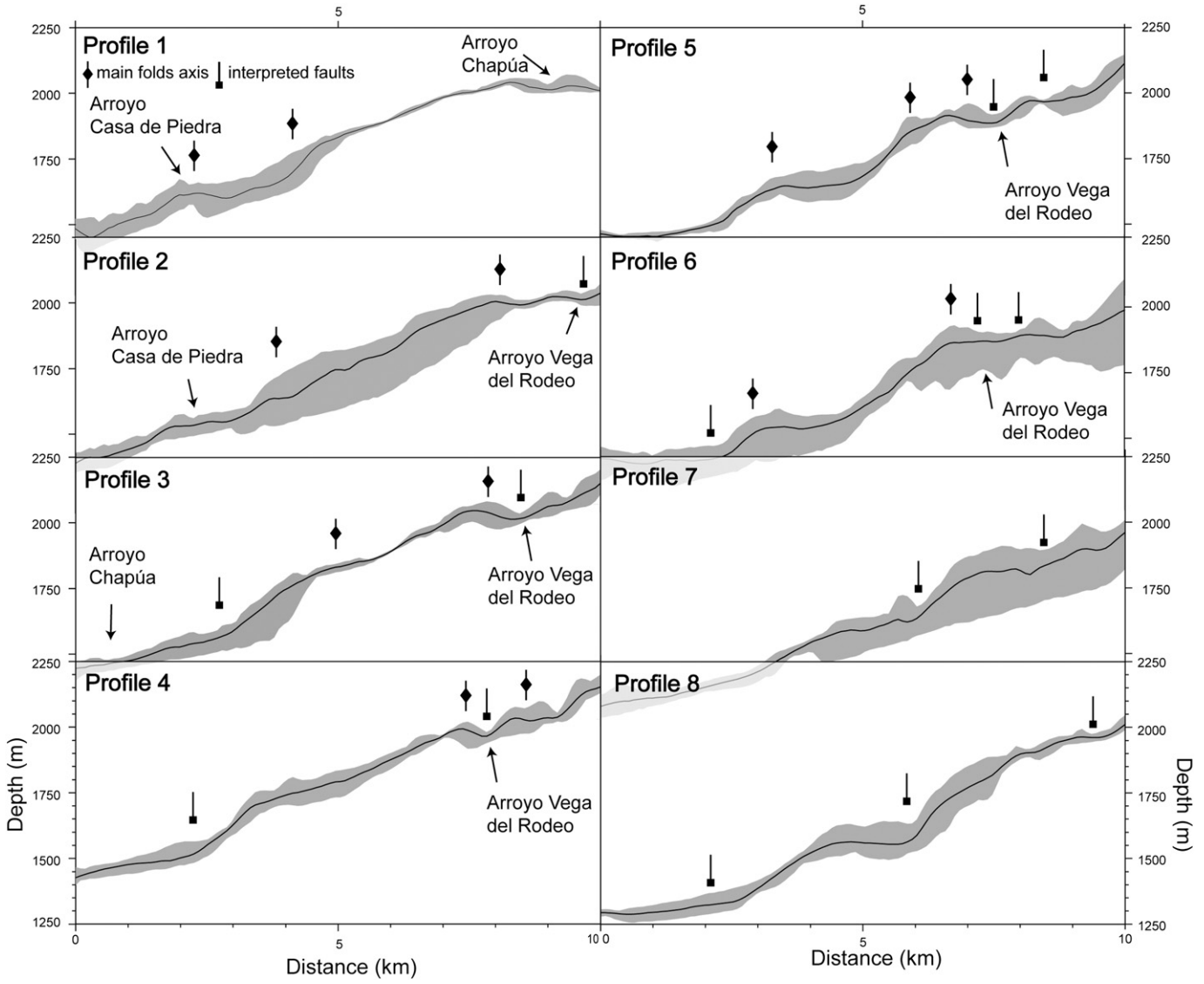

Fig. 12. Swath profiles across the western slope of the Tromen volcanic plateau, representing the maximum, minimum and mean data of the topography and location of main recognized neotectonic structures (see location in Fig. 11).

negative concavity value for the three sections (θ: −0.41). Moreover, Profile III — Arroyo Los Molles has a very concave/steep upper profile segment above the knickpoint, since its headwaters start on the flank of a young anticline. Contrastingly, V — Arroyo Blanco does not show any significant variations in the channel slope, with concavity values (θ) of 0.32 and 0.31 (Fig. 11c).

Analyzing concavity values across the studied profiles, a series of preliminary conclusions can be drawn. Negative concavity values (II — Arroyo Chapúa and IV — Arroyo Vega del Rodeo) are found in river profiles affected by neotectonic structures. In contrast, Arroyo Blanco and Arroyo Molles present higher concavity values nearer to the reference concavity (0.45). An exception to this is the I — Arroyo Casa de Piedra, which has a low concavity suggesting that is not experiencing as much tectonic forcing as the other streams with higher concavities, in spite of crossing neotectonic structures.

The profiles I, II and IV would be in transient states of disequilibrium as a consequence of emersion of active deformation (Fig. 11c).

Swath profiles were calculated across the western slope of the Tromen volcanic plateau representing the average of the maximum, minimum, and mean data of the topography along the profiles (Fig. 12). These allow visualization of the topographic variations, potentially related to neotectonic deformation, beyond the channels, that can be easily correlated through the different profiles.

Northern profiles, from 2 to 4, show common characteristics, with an irregular shape in their eastern section, a west-dipping central section and a western step (Fig. 12). The eastern irregularities are interpreted as being related to a neotectonic anticline bounded by a normal fault by its eastern side (Fig. 9; Vega del Rodeo fault), while the western step coincides with the Chapúa anticline. Southern profiles, from 5 to 8, show a roughened eastern section, similar to the previous profiles, an intermediate step (absent to the north), and finally a western step common to all sections (Fig. 12). The intermediate step in profiles 5 and 6 coincides with a neotectonic anticline, whereas to the south, in profiles 7 and 8, it is related to a west-dipping normal fault.

5. Discussion

This work describes a Pleistocene deformational belt that is located in the retroarc zone of the Southern Central Andes affecting the western slope of the Tromen volcanic plateau. This belt is located to the east of the Antiñir Copahue fault system (ACFS) which constitutes the northern prolongation of the Liquiñe Ofqui fault system (LOFS), both running through the Andean arc front for more than 1000 km from the triple junction between Antarctica, South America and Nazca plates at ~46° 30′S to ~37°S (Lavenu and Cembrano, 1999). Their position along the arc front is interpreted to be linked to the thermal weakening of the lower crust imposed by the emplacement of magmas produced at the asthenospheric wedge. This would allow concentration of lateral displacements and contraction, imposed by the convergence between the Nazca and South American plates, at the western section of the fold and thrust belt.

The described neotectonic structures in the western Tromen volcanic plateau constitute reactivations of specific parts of the Malargüe fold and thrust belt (Fig. 13). Additionally, morphometric analyses through the fluvial network permit recognition of a non-equilibrium state for most of the fluvial channels. However, part of the non-equilibrium state of the smaller channels could be the result of a resistant caprock (basalt) that would inhibit the migration of knickpoints. These channels will take longer to adjust to imposed uplift patterns than channels III — Arroyo Los Molles and V — Arroyo Blanco since they have less stream power.

The northern Tromen plateau area, along the Arroyo Chapúa, shows the broadest thin-skinned frontal section (Fig. 13), where Pleistocene ignimbrites and lava flows were deformed in two contractional stages. This section coincides with the area of maximum fluvial incision through the plateau, which is interrupted to the east by the Vega del Rodeo normal fault. This structure is branched into a series of minor synthetic traces that provoke the alternation of topographic lows and highs, corresponding to anticlines and synclines with a local *en echelon* distribution. In this zone, NE extensional and NW to NNW contractional structures coexist limited to a narrow strip of deformation, which is interpreted to be related to certain

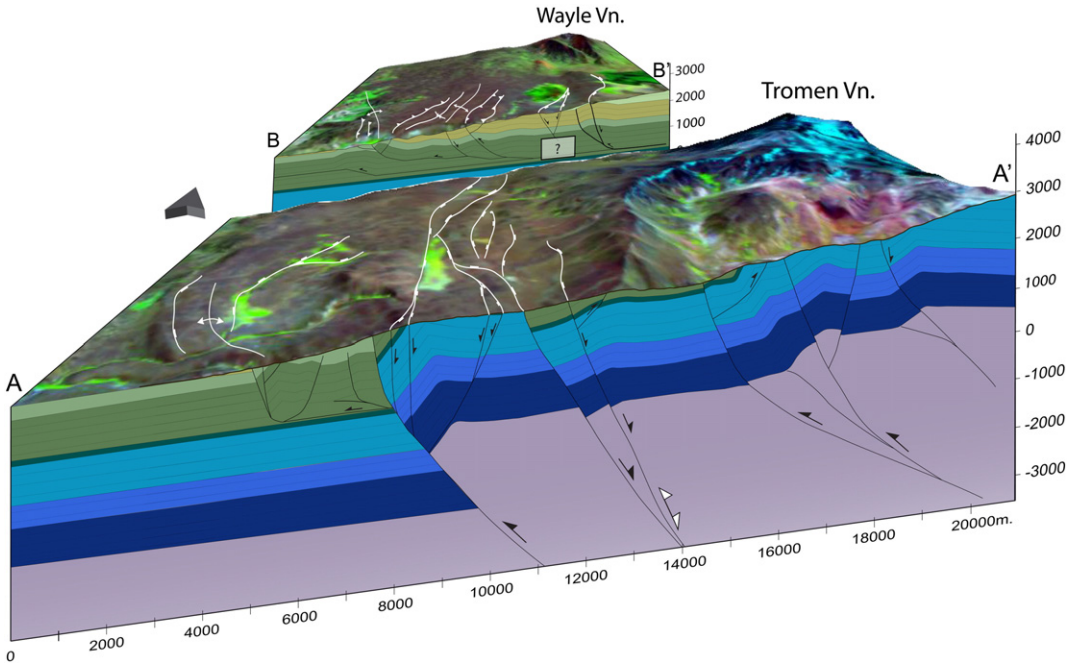

Fig. 13. Structural cross-sections of the Arroyo Blanco (A–A′) and Arroyo Chapúa (B–B′) in a 3D perspective produced by a DEM with TM image draped on top of it. Neotectonic structures are highlighted in white over the topography. Note that in the northern profile there is a broader active thin-skinned sector that narrows to the south where is replaced by prominent neotectonic basement structures.

amounts of dextral strike-slip displacements associated with shortening (Figs. 13, 14).

Morphometric analysis of the fluvial network complemented with morphological observations have allowed us to establish an evolutionary model for the area bounded between the Arroyo Chapúa in the north and the Arroyo Blanco in the south. Deflected channels and wind gaps are indicative of a reorganization of the fluvial drainage pattern, where the rivers are forced to change their original course by growing Pleistocene structures. In some cases these have migrated laterally towards the tips of the uplifting areas, where they form confluences with transverse rivers (Fig. 15). Through this reorganization associated with the Pleistocene orogenic uplift, the fluvial network changes its pattern from a radial fluvial network, typical of volcanic edifices, to a parallel — to the neotectonic structure fluvial network (Fig. 15).

For this analysis we correlate wind gaps with abandoned channels, determining the geometry of the fluvial network prior to the uplift of two anticlines that are included in the eastern neotectonic structures (Fig. 15). Most of the gorges crossing the anticline axis are described as wind gaps since these are now totally disconnected from the active fluvial network. However, to the south, a gorge affecting the nose of an anticline maintains a connection with upstream and downstream channels, indicating ongoing uplift. Thus, we interpret a southward progression of the anticline crest which deflects upstream channels to their final confluence with the Arroyo Blanco in the south (Fig. 15).

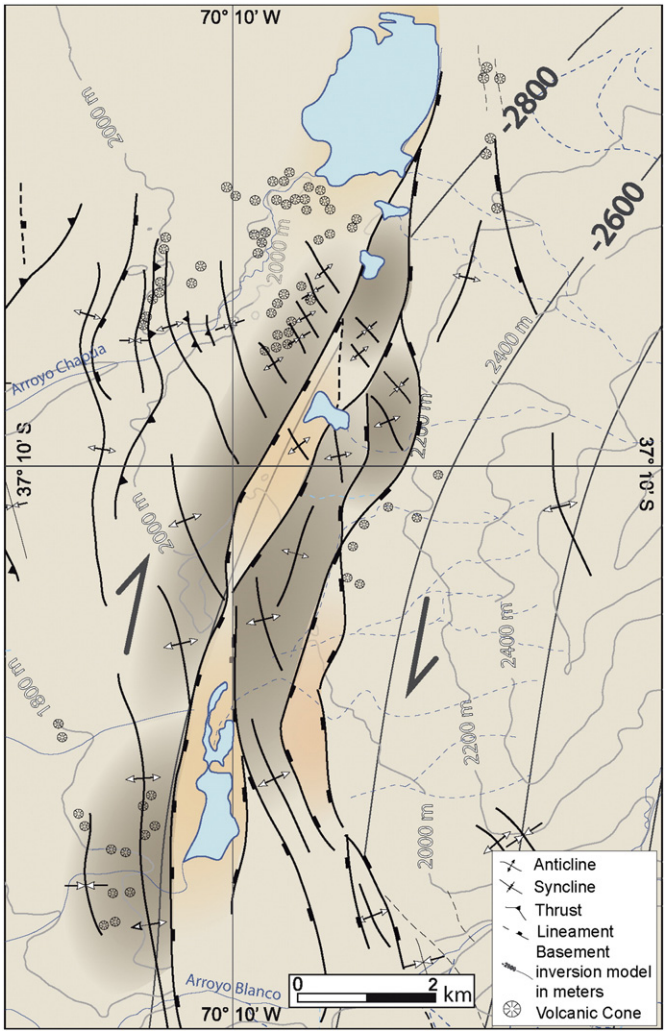

Fig. 14. Eastern neotectonic structures described in the western slope of the Tromen volcanic plateau: Note a general pattern of NW- to NNW-trending structures that absorb contraction, and NE structures that accommodate extension. This general arrangement is interpreted to be associated with a right-lateral component of this deformational front.

In a more regional analysis, 3D inversion of MT array data reveals a complex lower lithospheric and asthenospheric structure beneath the Tromen and Payenia volcanic plateaus (Burd et al., 2014) (Fig. 16). An asthenospheric anomaly, emerging from the 410-km-mantle discontinuity, is spatially associated with the development of the Payenia volcanic plateau. Thus, this volcanic plateau, and particularly the Tromen volcanic plateau, are identified as plume-related features (Burd et al., 2014). Particularly, beneath the western slope of the Tromen volcanic plateau, where neotectonic deformation has been described, this anomaly becomes shallower than 40 km (Fig. 16). Therefore, neotectonic deformation affecting the mid-sections of the Malargüe fold and thrust belt could be related to thermal weakening of the upper crust due to the development of an asthenospheric anomaly.

This process could explain why the retroarc zone is presently absorbing shortening associated with amounts of right lateral displacements, similarly to the LOFS and ACFS to the south and west, respectively (Fig. 16). Strain partitioning, linked to the oblique convergence between Nazca and South American plates, at the latitudes of this study would differ substantially with respect to the situation in the south. While between 46–38°S right-lateral displacements are absorbed at the arc zone where the crust is thermally debilitated due to magmatic addition, north of these latitudes these lateral displacements are absorbed at the retroarc zone where the crust is intruded by magmas coming from an impacting plume, as 3D inversion of MT array data reveals. Localized out-of-sequence neotectonic deformation and related modifications to the fluvial network could therefore be in association with these sublithospheric phenomena.

Note that both systems are developed in an out-of-sequence order with respect to the eastern-frontal structures developed through Cretaceous and Cenozoic times. Neotectonic systems accommodate contractional and right-lateral displacements imposed by the oblique convergence between the Nazca and South American plates.

6. Conclusions

Contractional structures associated with limited amounts of strike-slip displacements are affecting Pleistocene retroarc volcanic rocks and the fluvial network, as indicated in this and previous works. From this study, a connection between these structures and pre-Miocene deformations is established. A new Ar–Ar age and described relations between deformed strata show that at least two deformational stages have shaped this neotectonic front in Pleistocene times. An analysis of the fluvial network and morphotectonic evidence points to a present reactivation of the structure.

Neotectonics in the area would constitute a late reactivation of a pre-Miocene doubly vergent structure associated at depth with a contractional basement wedge. Its location indicates that the Malargüe fold and thrust belt would have reactivated through out-of-sequence structures, leaving to the east a fossilized sector. Location of this neotectonic front, further to the east of previously recognized neotectonic structures along the LOFS and ACFS, could be controlled by the development of an asthenospheric upwelling beneath the western Tromen volcanic plateau. This work constitutes additional evidence of the control that would be exerted by a thermally weakened crust in the reactivation of previous sections of the southern Andes, explaining the occurrence of out-of-sequence deformation and local modification of the original fluvial network.

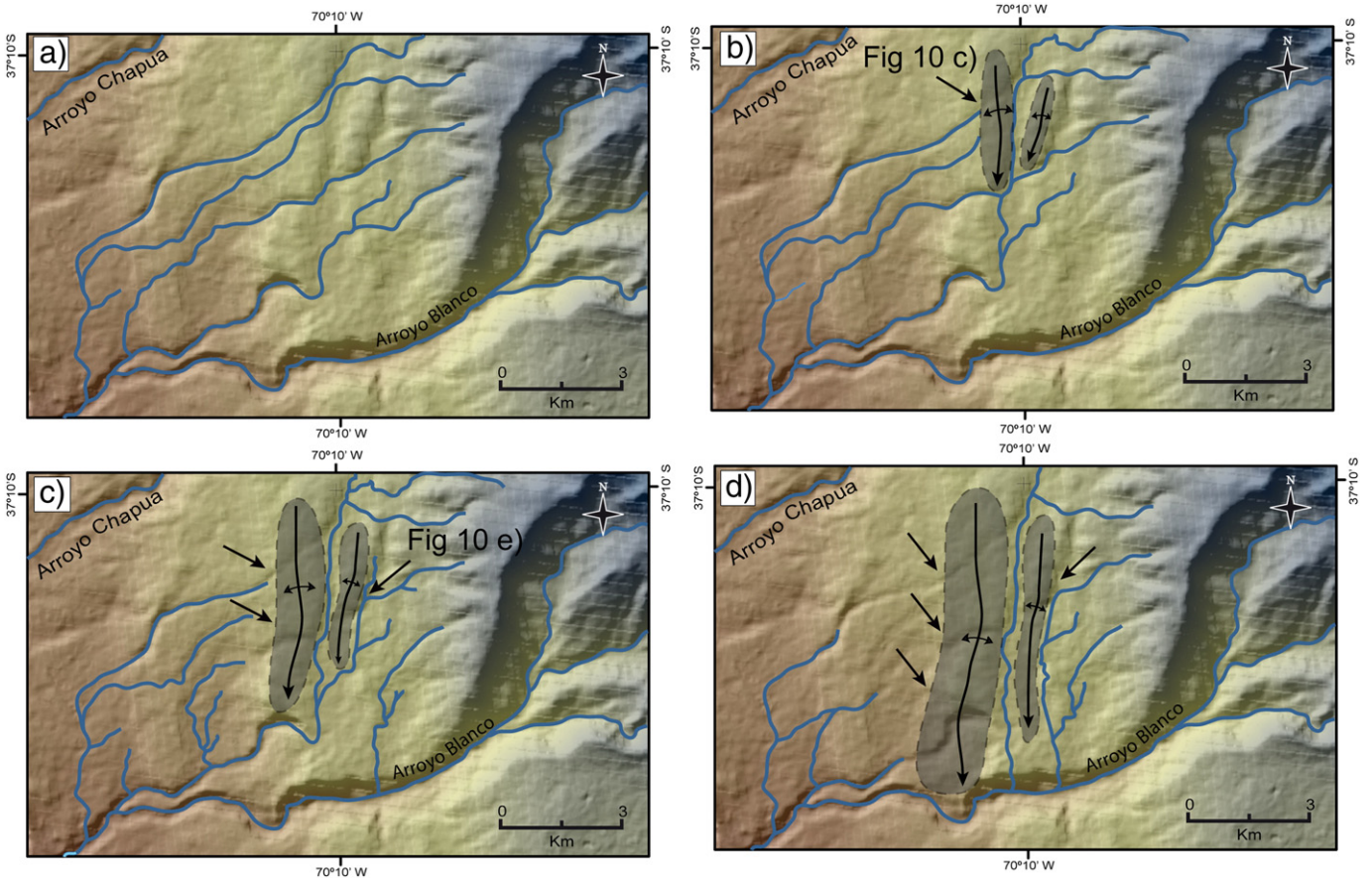

Fig. 15. Drainage evolutionary model of the western slope of the Tromen volcanic plateau. Black arrows indicate wind gaps, while gray-shaded ellipsoids represent the uplifted neotectonic anticlines. a) Inferred drainage pattern prior to the uplift of the identified neotectonic structures, draining from the NE to SW, after correlating wind gaps with dissected channels. b) Evolution of the drainage pattern during the first stage of anticline development. One wind gap and two dissected channels would be associated with this stage. c) Present drainage pattern with described wind gaps localized at the mid- part of both neotectonic anticlines. d) Hypothetical future drainage pattern following direction of propagation of the anticlines seen in the first stages, when rivers would be forced to migrate to the tips of the uplifting topography.

Acknowledgments

The new slice of the 3D electrical resistivity model used in this paper was provided to us by John Booker of the Dept. of Earth and Space Sciences of the University of Washington. We also acknowledge Peter Cobbold for discussion in the field. We thank Midland Valley Ltd. for providing us the academic licenses of the Move® software. This work was funded by UBACYT 20020110100019, PIP 11220110100506, PICT-2012-1490. This is the contribution R-151 of the Instituto de Estudios Andinos Don Pablo Groeber (UBA-CONICET).

Appendix A. Supplementary data

Supplementary data to this article can be found online at http://dx.doi.org/10.1016/j.geomorph.2014.12.022.

References

Backé, G., Hervouet, Y., Dhont, D., 2006. Cenozoic extension vs compression in the central Neuquén Basin (37°–36° S, Argentina). Backbone of the Americas Patagonia to Alaska. Geological Society of America, Abstract with programs, Special meeting, p. 111.

Brooks, B.A., Bevis, M., Smalley, R., Kendrick, E., Manceda, R., Lauría, E., Maturana, R., Araujo, M., 2003. Crustal motion in the Southern Andes (26°–36°S): do the Andes behave like a microplate? Geochem. Geophys. Geosyst. 4 (10). http://dx.doi.org/10.1029/2003GC000505.

Burbank, D., Anderson, R., 2012. Tectonic Geomorphology. Blackwell Science, p. 274.

Burd, A.I., Booker, J.R., Mackie, R., Favetto, A., Pomposiello, M.C., 2014. Three-dimensional electrical conductivity in the mantle beneath the Payún Matrú Volcanic Field in the Andean back-arc of Argentina near 36.5° S: decapitation of a mantle plume by resurgent upper mantle shear during slab steepening. Geophys. J. Int. http://dx.doi.org/10.1093/gji/ggu145.

Burd, A.I., Booker, J.R., Pomposiello, M.C., Favetto, A., Larsen, J., Giordanengo, G., Orozco Bernal, L., 2008. Electrical conductivity beneath the Payún Matrú volcanic field in the Andean back-arc of Argentina near 36.5°S: insights into the magma source. 7th International Symposium on Andean Geodynamics, Nice, France, Extended Abstractspp. 90–93.

Cembrano, J., Lara, L., 2009. The link between volcanism and tectonics in the southern volcanic zone of the Chilean Andes: a review. Tectonophysics 471, 96–113. http://dx.doi.org/10.1016/j.tecto.2009.02.038.

Cembrano, J., Lavenu, A., Reynolds, P., Arancibia, G., Lopéz, G., Sanhueza, A., 2002. Late Cenozoic transpressional ductile deformation north of the Nazca–South America–Antarctica triple junction. Tectonophysics 354, 289–314.

Charrier, R., Pinto, L., Rodríguez, M.P., 2007. Tectonostratigraphic Evolution of the Andean Orogen in Chile. In: Moreno, T., Gibbons, W. (Eds.), Geología de Chile. The Geological Society, London, pp. 21–114.

Costa, C.H., Audemard, M.F.A., Bezerra, F.H.R., Lavenu, A., Machette, M.N., París, G., 2006. An overview of the main quaternary deformation of South America. Rev. Asoc. Geol. Argent. 61, 461–479.

DeCelles, P.G., Ducea, M.N., Kapp, P., Zandt, G., 2009. Cyclicity in Cordilleran orogenic systems. Nat. Geosci. 2, 1–7. http://dx.doi.org/10.1038/ngeo469.

Egan, S., Budding, T., Kane, S.J., Williams, G., 1997. Three-dimensional modelling and visualisation in structural geology: new techniques for the restoration and balancing of volumes. Proceedings of the 1996 Geoscience Information Group Conference on Gelogical Visualitation, pp. 67–82.

Farías, M., Comte, D., Charrier, R., Martinod, J., David, C., Tassara, A., Tapia, F., Fock, A., 2010. Crustal-scale structural architecture in central Chile based on seismicity and

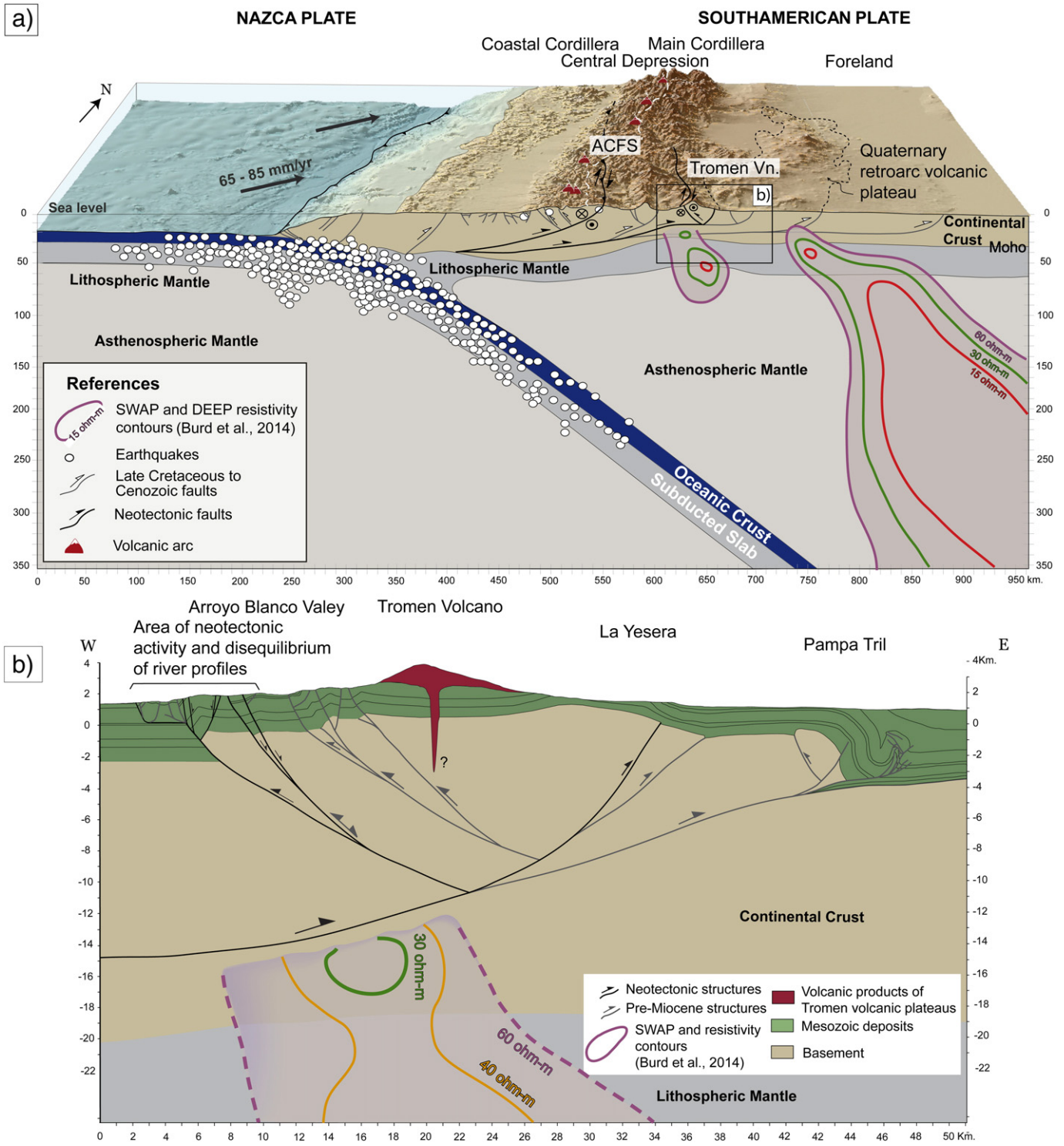

Fig. 16. a) Digital elevation model with cross- section that represents upper crustal structure at 37°S (see location in Fig. 1) (after Folguera et al., 2006; Zamora Valcarce et al., 2006; Sagripanti et al., 2012a, 2012b, 2013; Rojas Vera et al., 2014). Seismicity and geometry of the subduction zone are taken from Pesicek et al. (2012), while the resistivity anomalies in the mantle and lower crust are a cross-section of the 3D model of Burd et al. (2014) (the position of this slice is indicated in Fig. 2). Neotectonic structural systems are represented with thicker lines, along the arc front (ACFS) and the retroarc zone in the Tromen volcanic plateau area. b) Detail of the inferred mantle plume from the 3D model of Burd et al. (2014) impacting the lower crust and correlation with neotectonic deformation in the Tromen volcanic plateau.

surface geology: Implications for Andean mountain building. Tectonics 29. http://dx.doi.org/10.1029/2009TC002480.
Figueroa, A.M., Knott, J.R., 2010. Tectonic geomorphology of the southern Sierra Nevada Mountains (California): evidence for uplift and basin formation. Geomorphology 123, 34–45. http://dx.doi.org/10.1016/j.geomorph.2010.06.009.
Folguera, A., Ramos, V.A., 2009. Collision of the Mocha fracture zone and a <4 Ma old wave of orogenic uplift in the Andes (36°–38° S). Lithosphere 1, 364–369. http://dx.doi.org/10.1130/L66.1.
Folguera, A., Ramos, V.A., Hermanns, R.L., Naranjo, J., 2004. Neotectonics in the foothills of the southernmost central Andes (37°–38°S): evidence of strike-slip displacement along the Antiñir-Copahue fault zone. Tectonics 23. http://dx.doi.org/10.1029/2003TC001533 (n/a–n/a).
Folguera, A., Ramos, V.A., González Díaz, E.F., Hermanns, R.L., 2006. Miocene to Quaternary deformation of the Guañacos fold-and-thrust belt in the Neuquén Andes between 37° and 37°30′ S. In: Kay, S.M., Ramos, V.A. (Eds.), Evolution of an Andean Margin: A Tectonic and Magmatic View From the Andes to the Neuquén Basin (35°–39°S Lat).

Geological Society of America, Special Paper 407, pp. 247–266. http://dx.doi.org/10.1130/2006.2407(11).
Folguera, A., Bottesi, G., Zapata, T., Ramos, V.A., 2008. Crustal collapse in the Andean backarc since 2 Ma: Tromen volcanic plateau, Southern Central Andes (36°40′–37°30′S). Tectonophysics 459, 140–160. http://dx.doi.org/10.1016/j.tecto.2007.12.013.
Galland, O., Hallot, E., Cobbold, P.R., Ruffet, G., de Bremond d'Ars, J., 2007. Volcanism in a compressional Andean setting: a structural and geochronological study of Tromen volcano (Neuquén province, Argentina). Tectonics 26. http://dx.doi.org/10.1029/2006TC002011.
Guzmán, C., Cristallini, E., Bottesi, G., 2007. Contemporary stress orientations in the Andean retroarc between 34°S and 39°S from borehole breakout analysis. Tectonics 26. http://dx.doi.org/10.1029/2006TC001958.
Hack, J.T., 1973. Stream profile analysis and stream-gradient index. J. Res. U. S. Geol. Surv. 1, 421–429.
Havestadt, B., 1752. Mapa geográfico y diario del Padre Bernardo Havestadt (itinerario). En el cual se detallan las provincias, ciudades, sitios, días y leguas que en los últimos meses del año 1751 y los primeros meses del año 1752 (Available at http://es.wikisource.org/wiki/).
Hermanns, R.L., Folguera, A., Penna, I.M., Fauqué, L., Niedermann, S., 2011. Landslide dams in the Central Andes of Argentina (northern Patagonia and the Argentine northwest). In: Evans, S.G., Hermanns, R.L., Strom, A., Scarascia Mugnozza, G. (Eds.), Lecture Series in Earth Sciences. Natural and Artificial Rockslide Dams. Springer, Berlin, pp. 145–174.
Holmberg, E., 1975. Descripción geológica de la hoja 32c - Buta Ranquil - Provincia Mendoza-Neuquén, Boletín 15. ed. Servicio Geológico Minero Argentino, Buenos Aires.
Howard, A., Kerby, G., 1983. Channel changes in badlands. Geol. Soc. Am. 94, 739–752.
Jordan, T.E., Isacks, B.L., Allmendinger, R.W., Brewer, J.A., Ramos, V.A., Clifford, J.A., 1983. Andean tectonics related to geometry of subducted Nazca plate. Geol. Study Am. Bull. 94, 341–361.
Jordan, T.E., Burns, W.M., Veiga, R., Pángaro, F., Copeland, P., Kelley, S., Mpodozis, M.C., 2001. Extension and basin formation in the southern Andes caused by increased convergence rate: a mid-Cenozoic trigger for the Andes. Tectonics 20, 308–324.
Kane, S., Williams, G., Buddin, T., 1997. Flexural-slip based restoration in 3D, a new apprach. 1997 AAPG Annual Convention. Bakrsfield, California.
Kay, S.M., 2002. Tertiary to recent transient shallow subduction zones in the Central and Southern Andes. XV Congreso Geológico Argentino. Calafate, pp. 282–283.
Kay, S.M., Burns, W.M., Copeland, P., Oscar, M., 2006. Upper Cretaceous to Holocene magmatism and evidence for transient Miocene shallowing of the Andean subduction zone under the northern Neuquén Basin. In: Kay, S.M., Ramos, V.A. (Eds.), Evolution of an Andean Margin: A Tectonic and Magmatic View From the Andes to the Neuquén Basin (35°–39°S Lat). Geological Society of America, Special Paper 407, pp. 19–60. http://dx.doi.org/10.1130/2006.2407(02).
Kay, S.M., Jones, H.A., Kay, R.W., 2013. Origin of tertiary to recent EM- and subduction-like chemical and isotopic signatures in Auca Mahuida region (37°–38°S) and other Patagonian plateau lavas. Contrib. Mineral. Petrol. 166, 165–192. http://dx.doi.org/10.1007/s00410-013-0870-9.
Keller, A.E., Gurrola, L., Tierney, T., 1999. Geomorphic criteria to determine direction of lateral propagation of reverse faulting and folding. Geology 27, 515–518.
Kendrick, E.C., Bevis, M., Smalley, R.F., Cifuentes, O., Galban, F., 1999. Current rates of convergence across the central Andes: estimates from continuous GPS observations. Geophys. Res. Lett. 26, 541–544. http://dx.doi.org/10.1029/1999GL900040.
Kirby, E., Whipple, K., 2001. Quantifying differential rock-uplift rates via stream profile analysis. Geology 29, 415–418. http://dx.doi.org/10.1130/0091-7613(2001)029<0415.
Kirby, E., Whipple, K.X., 2012. Expression of active tectonics in erosional landscapes. J. Struct. Geol. 44, 54–75. http://dx.doi.org/10.1016/j.jsg.2012.07.009.
Kley, J., Monaldi, C.R., Salfity, J.A., 1999. Along-strike segmentation of the Andean foreland: causes and consequences. Tectonophysics 301, 75–94. http://dx.doi.org/10.1016/S0040-1951(98)90223-2.
Kozlowski, E., Manceda, Ramos, V.A., 1993. Estructura. In: Ramos, V.A. (Ed.), Geología y Recuersos Naturales de Mendoza. XII Congreso Argentino de Geología, II Congreso de Exploración de Hidrocarburos. Mendoza, pp. 235–256.
Kozlowski, E., Cruz, C.E., Sylwan, C., 1996. Geología estructural de la zona de Chos Malal. Cuenca Neuquina, Argentina. XIII Congreso Geológico Argentino, III Congreso de Exploración de Hidrocarburos. Buenos Aires, pp. 15–26.
Lagabrielle, Y., Suárez, M., Malavieille, J., Morata, D., Espinoza, F., Maury, R.C., Scalabrino, B., Barbero, L., de la Cruz, R., Rossello, E., Bellon, H., 2007. Pliocene extensional tectonics in the Eastern Central Patagonian Cordillera: geochronological constraints and new field evidence. Terra Nova 19, 413–424. http://dx.doi.org/10.1111/j.1365-3121.2007.00766.x.
Lavenu, A., Cembrano, J., 1999. Compressional- and transpressional-stress pattern for Pliocene and Quaternary brittle deformation in fore arc and intra-arc zones (Andes of Central and Southern Chile). J. Struct. Geol. 21, 1669–1691. http://dx.doi.org/10.1016/S0191-8141(99)00111-X.
Llambías, E.J., Palacios, M., Danderfer, J., 1982. Las erupciones Holocenas del Volcán Tromen (Provincia de Neuquén) y su significado en el perfil transversal E - O a la latitud 37° S. V Congreso Latinoamericano de Geología. Buenos Aires, pp. 537–545.
Llambías, E.J., Bertotto, G.W., Risso, C., 2010. El vulcanismo cuaternario en el retroarco de Payenia: una revisión. Rev. Asoc. Geol. Argent. 67, 278–300.
López-Escobar, L., Parada, M.A., Hickey-Vargas, R., Frey, F.A., Kempton, P.D., Moreno, H., 1995. Calbuco Volcano and minor eruptive centers distributed along the Liquiñe-Ofqui Fault Zone, Chile (41°–42° S): contrasting origin of andesitic and basaltic magma in the Southern Volcanic Zone of the Andes. Contrib. Mineral. Petrol. 119, 345–361. http://dx.doi.org/10.1007/BF00286934.
Marques, F.O., Cobbold, P.R., 2002. Topography as a major factor in the development of arcuate thrust belts: insights from sandbox experiments. Tectonophysics 348, 247–268. http://dx.doi.org/10.1016/S0040-1951(02)00077-X.
Melnick, D., Rosenau, M., Folguera, A., Echtler, H., 2006. Neogene Tectonics of the Western flank of the Neuquén Andes, 37°–39°30' S. In: Kay, S.M., Ramos, V.A. (Eds.), Evolution of an Andean Margin: A Tectonic and Magmatic View from the Andes to the Neuquén Basin (35°–39°S Lat). Geol. Soc. Am. 407. Special Paper, pp. 73–95.
Messager, G., Nivière, B., Martinod, J., Lacan, P., Xavier, J.-P., 2010. Geomorphic evidence for Plio-Quaternary compression in the Andean foothills of the southern Neuquén Basin, Argentina. Tectonics 29. http://dx.doi.org/10.1029/2009TC002609.
Oncken, O., Hindle, D., Kley, J., Elger, K., Victor, P., Schemmann, K., 2003. Deformation of the Central Andean Upper Plate System — facts, fiction, and constraints for plateau models. In: Brun, J.-P., Oncken, O., Weissert, H.H.D. (Eds.), The Andes. Springer, Berlin Heidelberg, pp. 1–25.
Pananont, P., Mpodozis, C., Blanco, N., Jordan, T.E., Brown, L.D., 2004. Cenozoic evolution of the northwestern Salar de Atacama Basin, northern Chile. Tectonics 23. http://dx.doi.org/10.1029/2003TC001595.
Pazzaglia, F.J., Gardner, T.W., Merritts, D.J., 1998. Bedrock fluvial incision and longitudinal profile development over geologic time scales determined by fluvial terraces. In: Wohl, E., Tinkler, K. (Eds.), River Over Rock: Fluvial Processes in Bedrock Channels. American Geophysical Union, pp. 207–235.
Penna, I.M., Hermanns, R.L., Niedermann, S., Folguera, A., 2011. Multiple slope failures associated with neotectonic activity in the Southern Central Andes (37°–37°30′S), Patagonia, Argentina. Geol. Soc. Am. Bull. 123, 1880–1895.
Pesicek, J.D., Engdahl, E.R., Thurber, C.H., DeShon, H.R., Lange, D., 2012. Mantle subducting slab structure in the region of the 2010 M8.8 Maule earthquake (30–40°S), Chile. Geophys. J. Int. 191, 317–324. http://dx.doi.org/10.1111/j.1365-246X.2012.05624.x.
Quezada, J., Bataille, K., 2008. Subduction partitioning evidenced by crustal earthquakes along the Chilean Andes. 7th International Symposium on Andean Geodynamics. Nice, pp. 413–416.
Radic, J.P., Rojas, L., Carpinelli, A., Zurita, E., 2002. Evolución tectónica de la cuenca terciaria de Cura-Mallín. Región cordillerana chileno argentina (36°30´- 39°00´S). XV Congreso Geológico Argentino 3. Calafate, pp. 233–237.
Ramos, V.A., 1998. Estructura del sector occidental de la faja plegada y corrida del Agrio, cuenca neuquina, Argentina. X Congreso Latinoamericano de Geología. Buenos Aires, pp. 105–110.
Ramos, V.A., 2010. The Grenville-age basement of the Andes. J. S. Am. Earth Sci. 29, 77–91. http://dx.doi.org/10.1016/j.jsames.2009.09.004.
Ramos, V.A., Aleman, 2000. Tectonics of the Andes. In: Cordani, U.G., Milani, E.J., Filho, T., Campos, D.A. (Eds.), Tectonic Evolution of South America, pp. 635–685.
Ramos, V.A., Folguera, A., 2005. Tectonic evolution of the Andes of Neuquén: constraints derived from the magmatic arc and foreland deformation. In: Veiga, G.D., Spalleti, L.A., Howell, J.A., Schwarz, E. (Eds.), The Neuquén Basin, Argentina: A Case Study in Sequence Stratigraphy and Basin Dynamics. The Geological Society of London, pp. 15–35.
Ramos, V.A., Folguera, A., 2011. Payenia volcanic province in the Southern Andes: an appraisal of an exceptional Quaternary tectonic setting. J. Volcanol. Geotherm. Res. 201, 53–64. http://dx.doi.org/10.1016/j.jvolgeores.2010.09.008.
Ramos, V.A., Zapata, T., Cristallini, E., Introcaso, A., 2004. The Andean thrust system — latitudinal variations in structural styles and orogenic shortening. In: McClay, K.R. (Ed.), Thrust Tectonics and Hydrocarbon Systems. AAPG Memoir 82, pp. 30–50.
Ramos, V.A., Litvak, V.D., Folguera, A., Spagnuolo, M., 2014. An Andean tectonic cycle: from crustal thickening to extension in a thin crust (34°–37°SL). Geosci. Front. 5, 351–367. http://dx.doi.org/10.1016/j.gsf.2013.12.009.
Ramos, V.A., Kay, S.M., 2006. Overview of the tectonic evolution of the southern Central Andes of Mendoza and Neuquen (35°– 39°S latitude). In: Kay, S.M., Ramos, V.A. (Eds.), Evolution of an Andean Margin: A Tectonic and Magmatic View from theAndes to the Neuquén Basin (35°–39°S Lat). Geol. Soc. Am. Special Paper 407, pp. 1–17.
Rojas Vera, E.A., Folguera, A., Gímenez, M., Martínez, P., Ruiz, F., Ramos, V.A., 2008. Evolución tectónica de la Fosa de Loncopué: Estructura del depocentro cuaternario del Huecú y su relación con la sedimentación y el volcanismo. Rev. Asoc. Geol. Argent. 64, 214–230.
Rojas Vera, E.A., Folguera, A., Zamora Valcarce, G., Bottesi, G.L., Ramos, V.A., 2014. Structure and development of the Andean system between 36°–39° S. J. Geodyn. 73, 34–52. http://dx.doi.org/10.1016/j.jog.2013.09.001.
Sagripanti, L., Bottesi, G., Kietzmann, D., Folguera, A., Ramos, V.A., 2012a. Mountain building processes at the orogenic front. A study of the unroofing in Neogene foreland sequence (37°S). Andean Geol. 39, 201–219.
Sagripanti, L., Rojas Vera, E.A., Guianni, G., Rusconi, F., Ruiz, F., Folguera, A., Ramos, V.A., 2012b. Transtensive to transpressive neotectonic reactivation of a fold and thrust belt: the Tromen volcanic plateau in the southern Central Andes. XIII Congreso Geológico Chileno. Antofagasta.
Sagripanti, L., Aguirre-Urreta, M.B., Folguera, A., Ramos, V.A., 2013. The Neocomian of Chachahuén (Mendoza, Argentina): evidence of a broken foreland associated with the Payenia flat-slab. In: Sepúlveda, S.A., Giambiagi, L.B., Moreiras, S.M., Pinto, L., Tunik, M., Hoke, G.D., Farías, M. (Eds.), Geodynamic Processes in the Andes of Central Chile and Argentina. Geological Society of London Special Publication 399. http://dx.doi.org/10.1144/SP399.9.
Siebert, L., Simkin, T., Kimberly, P., 2011. Volcanoes of the World. 3rd ed. Smithsonian Institution. University of California Press.
Snyder, N.P., Whipple, K.X., Tucker, G.E., Merritts, D.J., 2000. Landscape response to tectonic forcing: digital elevation model analysis of stream profiles in the Mendocino triple junction region, northern California. Geol. Soc. Am. Bull. 112, 1250–1263.
Søager, N., Holm, P.M., Llambías, E.J., 2013. Payenia volcanic province, southern Mendoza, Argentina: OIB mantle upwelling in a backarc environment. Chem. Geol. 349–350, 36–53. http://dx.doi.org/10.1016/j.chemgeo.2013.04.007.
Somoza, R., Ghidella, M.E., 2012. Late Cretaceous to recent plate motions in western South America revisited. Earth Planet. Sci. Lett. 331–332, 152–163. http://dx.doi.org/10.1016/j.epsl.2012.03.003.

Somoza, R., Zaffarana, C.B., 2008. Mid-Cretaceous polar standstill of South America, motion of the Atlantic hotspots and the birth of the Andean cordillera. Earth Planet. Sci. Lett. 271, 267–277. http://dx.doi.org/10.1016/j.epsl.2008.04.004.

Spagnuolo, M.G., Litvak, V.D., Folguera, A., Bottesi, G., Ramos, V.A., 2012. Neogene magmatic expansion and mountain building processes in the southern Central Andes, 36–37°S, Argentina. J. Geodyn. 53, 81–94. http://dx.doi.org/10.1016/j.jog.2011.07.004.

Vergani, G.D., Tankard, A.J., Belotti, H.J., Welsink, H.J., 1995. Tectonic evolution and paleogeography of the Neuquén Basin, Argentina. In: Tankard, J., Suarez, S.R., Welsink, J. (Eds.), Petroleoum Basin of South America. AAPG Memori 62, pp. 383–402.

Whipple, K.W., Tucker, G.E., 1999. Dynamics of the stream-power river incision model: implications for height limits of mountain ranges, landscape response timescale, and research needs. J. Geophys. Res. 104, 17,661–17,674.

Whipple, K.X., Hancock, G.S., Anderson, R.S., 2000. River incision into bedrock: mechanics and relative efficacy of plucking, abrasion and cavitation. Geol. Soc. Am. Bull. 112, 490–503.

Wobus, C., Whipple, K.X., Kirby, E., Snyder, N., Johnson, J., Spyropolou, K., Crosby, B., Sheehan, D., 2006. Tectonic from topography: procedures, promise, and pitfalls. In: Willett, S., Hovius, N., Brandon, M., Fisher, D. (Eds.), Tectonic, Climate and Landscape Evolution. Geological Society of America, Special Paper 398, pp. 55–74.

Zamora Valcarce, G., Zapata, T., 2005. Estilo estructural del frente de la faja plegada neuquina a los 37° S. VI Congreso de Exploracion y Desarrollo de Hidrocarburos. Mar del Plata, p. 16.

Zamora Valcarce, G., Zapata, T., Del Pino, D., Ansa, A., 2006. Structural evolution and magmatic characteristics of the Agrio fold-and-thrust belt. In: Kay, S.M., Ramos, V.A. (Eds.), Evolution of an Andean Margin: A Tectonic and Magmatic View From the Andes to the Neuquén Basin (35°–39°S Lat). Bull. Geol. Soc. Am, Special Paper 407, pp. 125–145. http://dx.doi.org/10.1130/2006.2407(06).

Zamora Valcarce, G., Zapata, T., Ramos, V.A., Rodríguez, F., Bernardo, M.L., 2009. Evolución tectónica del frente andino en neuquén. Rev. Asoc. Geol. Argent. 65, 192–203.

Zapata, T., Brissón, I., Dzelalija, F., 1999. La Estructura de la faja plegada y corrida andina en relación con el control del basamento de la Cuenca Neuquina. Boletín de informaciones Petroleras, pp. 112–121.

Zollner, W., Amos, A., 1973. Descripción geológica de la hoja 32b - Chos Malal - Provincia de Neuquén, Boletín 14. ed. Servicio Geológico Minero Argentino.